
**Microbeam analysis — Scanning
electron microscopy — Method for
evaluating critical dimensions by CD-
SEM**

*Analyse par microfaisceaux — Méthode d'évaluation des dimensions
critiques par CD-SEM*

STANDARDSISO.COM : Click to view the full PDF of ISO 21466:2019



STANDARDSISO.COM : Click to view the full PDF of ISO 21466:2019



COPYRIGHT PROTECTED DOCUMENT

© ISO 2019

All rights reserved. Unless otherwise specified, or required in the context of its implementation, no part of this publication may be reproduced or utilized otherwise in any form or by any means, electronic or mechanical, including photocopying, or posting on the internet or an intranet, without prior written permission. Permission can be requested from either ISO at the address below or ISO's member body in the country of the requester.

ISO copyright office
CP 401 • Ch. de Blandonnet 8
CH-1214 Vernier, Geneva
Phone: +41 22 749 01 11
Fax: +41 22 749 09 47
Email: copyright@iso.org
Website: www.iso.org

Published in Switzerland

Contents

	Page
Foreword	iv
Introduction	v
1 Scope	1
2 Normative references	1
3 Terms and definitions	1
4 Symbols and abbreviated terms	8
5 Generation of Model-based Library (MBL)	8
5.1 Basic components of a MBL simulator.....	8
5.1.1 Electron probe model.....	8
5.1.2 SE signal generation model.....	10
5.1.3 SE signal detection model.....	11
5.2 Model of specimen.....	12
5.2.1 Specimen structure and parameters.....	12
5.2.2 Specimen specification.....	15
5.2.3 Generation methods of specimen geometry.....	15
5.3 Monte Carlo simulation.....	15
5.3.1 Input parameters.....	15
5.3.2 Beam-specimen interaction.....	16
5.4 MBL file structure.....	16
5.4.1 Variable type and value.....	16
5.4.2 Model description file.....	20
5.4.3 Parameter specification file.....	21
5.4.4 Preparation of library data.....	21
5.4.5 MBL data structure.....	22
5.4.6 MBL data file format.....	22
6 Acquisition of a CD-SEM image	23
6.1 Acceptable image.....	23
6.2 Specimen tilt.....	23
6.3 Image quality.....	23
6.4 Selection of the field of view.....	23
6.5 CD-SEM image data file.....	23
7 CD determination	23
7.1 Determination of pixel size.....	24
7.2 Selection of the field of interest.....	24
7.3 Coordination and normalization.....	24
7.4 Matching procedure.....	25
7.4.1 Interpolation.....	25
7.4.2 Convolution.....	25
7.4.3 Matching.....	26
7.4.4 Averaging.....	30
8 Module functions and relationship	31
9 Uncertainty of CD measurement	33
Annex A (normative) Flow charts of procedures	35
Annex B (informative) Example of model description file	39
Annex C (informative) Example of parameter specification file	40
Annex D (informative) Example of CD evaluation	41
Bibliography	44

Foreword

ISO (the International Organization for Standardization) is a worldwide federation of national standards bodies (ISO member bodies). The work of preparing International Standards is normally carried out through ISO technical committees. Each member body interested in a subject for which a technical committee has been established has the right to be represented on that committee. International organizations, governmental and non-governmental, in liaison with ISO, also take part in the work. ISO collaborates closely with the International Electrotechnical Commission (IEC) on all matters of electrotechnical standardization.

The procedures used to develop this document and those intended for its further maintenance are described in the ISO/IEC Directives, Part 1. In particular, the different approval criteria needed for the different types of ISO documents should be noted. This document was drafted in accordance with the editorial rules of the ISO/IEC Directives, Part 2 (see www.iso.org/directives).

Attention is drawn to the possibility that some of the elements of this document may be the subject of patent rights. ISO shall not be held responsible for identifying any or all such patent rights. Details of any patent rights identified during the development of the document will be in the Introduction and/or on the ISO list of patent declarations received (see www.iso.org/patents).

Any trade name used in this document is information given for the convenience of users and does not constitute an endorsement.

For an explanation of the voluntary nature of standards, the meaning of ISO specific terms and expressions related to conformity assessment, as well as information about ISO's adherence to the World Trade Organization (WTO) principles in the Technical Barriers to Trade (TBT), see www.iso.org/iso/foreword.html.

This document was prepared by Technical Committee ISO/TC 202, *Microbeam analysis*, Subcommittee SC 4, *Scanning electron microscopy (SEM)*.

Any feedback or questions on this document should be directed to the user's national standards body. A complete listing of these bodies can be found at www.iso.org/members.html.

Introduction

Nanostructures need strict dimensional control to meet the demands of the semiconductor industry. Critical dimension (CD) is the minimum size of a feature on an integrated circuit that impacts the electrical properties of the device, whose value represents the level of complexity of manufacturing. At nanometer scale, measurement uncertainty control becomes more difficult with much smaller dimensions. A determination method with algorithm for accurate measurement is a key for CD valuation. CD-SEMs (critical dimension scanning electron microscopes) are one of the main tools for CD measurement in semiconductor manufacturing processes, where secondary electrons (SEs) are the signal source for CD-SEM imaging of surface structure. The CD-SEM image displays the structure geometry, but the image contrast is not a perfect representation of the structure morphology. The detected intensity linescan profile of SE signals carries the information about the sample shape and composition, beam size and shape and the information volume generated by the electron beam-solid interaction. Restricted by the physical mechanism in the processes of SE signal generation and emission, the SE signal profiles show an edge effect which leads to difficulty for accurate CD value determination with image contrast. A reliable CD determination method which bases on physical principle of SE signal emission is necessary.

Many factors, for example the specimen chemical composition, structural geometric parameters, beam conditions and other specimen/instrument factors (charging, vibration and drift), can affect CD-SEM image contrast and hence the CD measurement result. Topographic contrast in the SE mode is resulted from the enhanced SE emission from an edge as well as tilted local surface in relative to the incident beam. The quantitative description of contrast or SE intensity profile is crucial in CD metrology.

The physical mechanisms that dominate quantitative measurements by CD-SEM have been well understood. The CD determination algorithm is based on physical modelling of SE generation and emission and gives adequate consideration of the influence of various experimental factors during electron beam-specimen interaction. This document employs the model-based library (MBL) method for accurate CD determination by CD-SEM. MBL is superior to simpler, unsophisticated, arbitrary methods that disregard the physics of signal generation, and report only a meagre number, potentially with unacceptably high bias. MBL uses the whole waveform of the signal, so it can provide results with less bias and better size and shape accuracy. Once the library is set up, there is essentially no time penalty for using MBL. Construction of MBL is done with a Monte Carlo (MC) simulator which is considered as an excellent approach to take into account of every possible physical factor that may affect signal intensity and shape of linescan profiles. The library generation can be sped up tremendously by suitable multicore computing environment and MC software that is optimized for a specific measurand. Such obtained MBL relates the measured signal linescan profiles to both specimen parameters and instrumental parameters. The library database is consisted of the simulated SE linescan profiles, having a one-to-one correspondence to a specified value of parameter set. By matching the shape of SE linescan profile taking from a measured CD-SEM image with those simulated beforehand and stored in a MBL database, the best fitted CD values used in MC modelling are selected.

[STANDARDSISO.COM](https://standardsiso.com) : Click to view the full PDF of ISO 21466:2019

Microbeam analysis — Scanning electron microscopy — Method for evaluating critical dimensions by CD-SEM

1 Scope

This document specifies the structure model with related parameters, file format and fitting procedure for characterizing critical dimension (CD) values for wafer and photomask by imaging with a critical dimension scanning electron microscope (CD-SEM) by the model-based library (MBL) method. The method is applicable to linewidth determination for specimen, such as, gate on wafer, photomask, single isolated or dense line feature pattern down to size of 10 nm.

2 Normative references

There are no normative references in this document.

3 Terms and definitions

For the purposes of this document, the following terms and definitions apply.

ISO and IEC maintain terminological databases for use in standardization at the following addresses:

- ISO Online browsing platform: available at <https://www.iso.org/obp>
- IEC Electropedia: available at <http://www.electropedia.org/>

3.1

critical dimension

CD

<for a line> minimum geometrical feature size limited by the photolithography technology used for the fabrication process

3.2

CD metrology

measurement of the width of line and space for a trapezoidal line structure model

Note 1 to entry: Extended CD metrology includes the measurement of top CD, middle CD, bottom CD, height, sidewall angle, top rounding and foot rounding. [Figure 1](#) shows schematically the definition of CDs.

Note 2 to entry: The term “top rounding” indicates a circular arc at the top corner, which is tangent to the top surface and side surface of a trapezoidal line, and whose value is represented by the circular radius.

Note 3 to entry: The term “foot rounding” indicates a circular arc at the bottom corner, which is tangent to the bottom surface and side surface of a trapezoidal line, and whose value is represented by the circular radius.

Note 4 to entry: More frequently CD represents the size of a feature on an integrated circuit or transistor that impacts the electrical properties of the device.

Note 5 to entry: Top rounding and foot rounding are not designed parameters.

3.3
critical-dimension scanning electron microscope
CD-SEM

special instrument for measuring *CDs* (3.1) of the fine patterns formed on a semiconductor wafer by producing magnified *images* (3.4) of a *specimen* (3.19) by scanning its surface with a focused electron beam

Note 1 to entry: It is mainly used in the manufacturing lines of electronic devices of semiconductors and optimized for dimensional metrology task, and differs from a general-purpose laboratory SEM in several aspects: 1. primary electron beam irradiates the sample at normal or nearly normal incidence condition; 2. the measurement repeatability around 1 % 3σ of the measurement width is guaranteed by improving magnification calibration to the maximum extent; 3. fine pattern measurements on the wafer are automated.

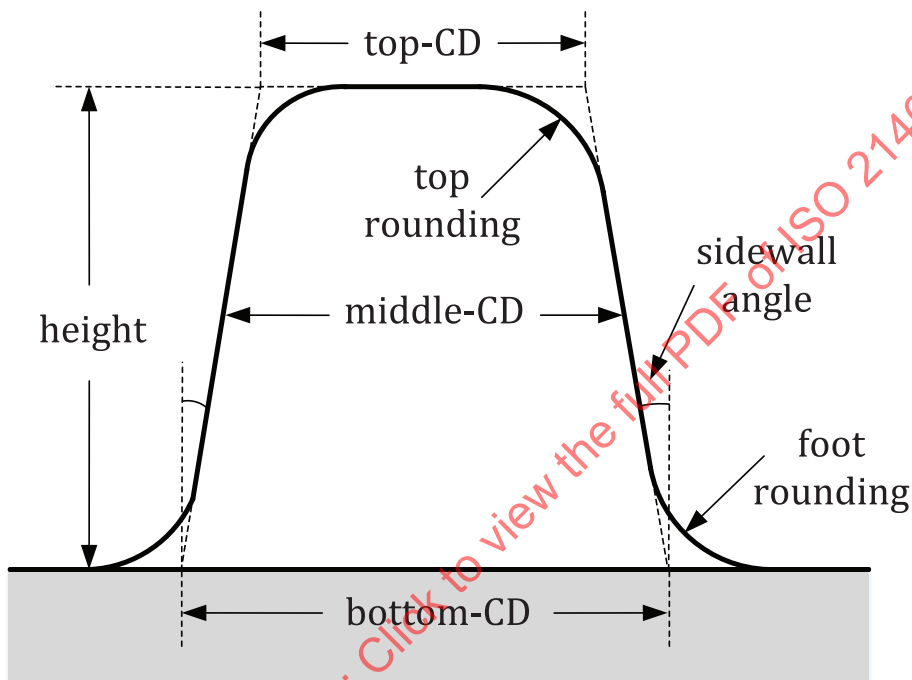


Figure 1 — Definition of CDs: top CD, middle CD, bottom CD, height, sidewall angle, top rounding and foot rounding

3.4
image

two-dimensional representation of the *specimen* (3.19) surface generated by SEM

Note 1 to entry: A photograph of a specimen taken using an SEM is a good example of an image.

[SOURCE: ISO 16700:2016, 3.2]

3.5
SEM imaging

action of forming an *image* (3.4) by a mapping operation that collects electron signals emitted from the *specimen* (3.19) surface and passes the digital signal intensity information into the storage devices

3.6
SE image

scanning (3.9) of electron beam *images* (3.4) in which the signal is derived from a detector that selectively measures *secondary electrons* (3.20) (electrons having energies less than 50 eV) and is not directly sensitive to backscattered electrons

Note 1 to entry: Intensity of digital CD-SEM image is adjusted to 8 bit (or other) depth of grayscale and does not equal to the detected physical number of secondary electron signals.

[SOURCE: ISO 23833:2013, 4.4.11, modified — Note 1 to entry added.]

3.7

electron probe

electron beam focused by the electron optical system onto the *specimen* (3.19)

[SOURCE: ISO 22493:2014, 7.1]

3.8

electron probe size

beam size

beam width

diameter of a circle that contains 50 % of the total *electron probe* (3.7) current

Note 1 to entry: For an ideal Gaussian probe shape in the radial direction:

$$\tilde{G}(r|\sigma_b) = \frac{1}{2\pi\sigma_b^2} \exp\left(-\frac{r^2}{2\sigma_b^2}\right) \quad (1)$$

the electron probe size is determined by the standard deviation (σ_b) as $d_p = 2\sqrt{2\ln 2} \sigma_b$, which is equal to the full width at half maximum (FWHM) of the Gaussian peak.

3.9

scanning

action of obtaining time-controlled movement of the *electron probe* (3.7) on the *specimen* (3.19) surface

3.10

linescan profile

signal intensity as function of coordinate along a straight line across an *image* (3.4)

3.11

focusing

aiming the electrons onto a particular point using an electron lens

[SOURCE: ISO 22493:2014, 3.1.4]

3.12

convergence angle

half-angle of the cone of the beam electrons converging onto the *specimen* (3.19)

[SOURCE: ISO 22493:2014, 7.1.1]

3.13

working distance

distance between the lower surface of the pole piece of the objective lens and the *specimen* (3.19) surface

Note 1 to entry: In the past, this distance was defined as the distance between the principal plane of the objective lens and the plane containing the specimen surface.

[SOURCE: ISO 22493:2014, 4.5.2]

3.14

charging effect

distortion of signal intensity in *SEM imaging* (3.5) of non-conductive *specimens* (3.19) due to accumulation of spatial charges in homogeneously distributed and hence the establishment of surface electric potential, which alters primary electron incidence (including landing energy and position) and all emitted electron signal properties

Note 1 to entry: The effect is a time dependent phenomenon and mainly related to current density and beam energy.

3.15

pixel

smallest discrete *image* (3.4) data element that constitutes an SEM image

[SOURCE: ISO 22493:2014, 5.2.4]

3.16

pixel size

length of the *pixel* (3.15), measured at a *specimen* (3.19) surface

Note 1 to entry: For a square or circular pixel, the horizontal and vertical pixel sizes should be the same.

[SOURCE: ISO 22493:2014, 5.2.5]

3.17

contrast

difference in signal intensities between two arbitrarily chosen points of interest in the *image* (3.4) field

3.18

graphics file format

archival digital format for storing the contents of the frame store

Note 1 to entry: The most popular image file formats are: bitmap (BMP), graphics interchange format (GIF), tagged image format (TIF) and joint photographic experts group (JPG). The TIF format can preserve all data and keeps the size of each pixel in its header. Consequently, this format is preferred to maintain the integrity of the images.

[SOURCE: ISO 22493:2014, 5.6.4, modified — “TIF format is the scientific format that preserves” is changed to “TIF format can preserve”, admitted term “image file format” removed.]

3.19

specimen

sampled material designated to be examined or analysed

[SOURCE: ISO 22493:2014, 4.5]

3.20

secondary electron

SE

electron emitted from the *specimen* (3.19) by the excitation of loosely bound valence electrons of the specimen in electron *inelastic scattering* (3.31) events and in a cascade production process as a result of bombardment by excitation beams, e.g. electrons, ions and photons

Note 1 to entry: By convention, an emitted electron with energy lower than 50 eV is considered as a secondary electron when primary energy is above 50 eV.

3.21

SE yield

total number of *secondary electrons* (3.20) per incident electron

[SOURCE: ISO 22493:2014, 3.4.1]

3.22

SE angular distribution

distribution of *secondary electrons* (3.20) as a function of their emitting angles relative to the surface normal

[SOURCE: ISO 22493:2014, 3.4.2]

3.23

SE energy distribution

distribution of *secondary electrons* (3.20) as a function of their emitting energies above the vacuum level

[SOURCE: ISO 22493:2014, 3.4.3, modified — added “above the vacuum level”]

3.24

SE tilt dependence

effect on *secondary electrons* (3.20) of the *specimen* (3.19) tilt which accompanies a change in incident beam angle

[SOURCE: ISO 22493:2014, 3.4.5]

3.25

Monte Carlo simulation

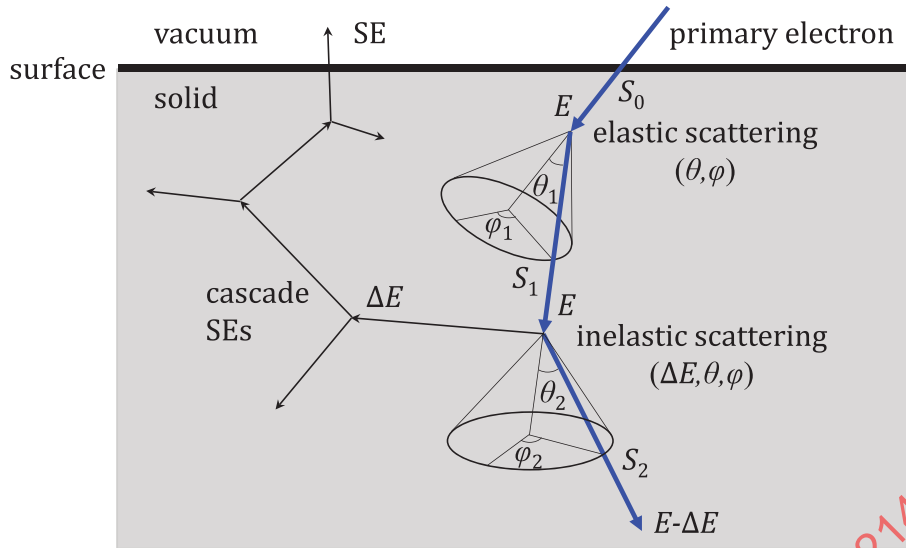
MC simulation

broad class of computational algorithms that uses statistical sampling techniques to obtain numerical results of a math model (Eckhardt 1987)

Note 1 to entry: The calculation models stochastic physical processes in the electron beam-specimen interaction and SEM image formation (Shimizu 1992; Joy 1995). The incident electron beam strikes the surface of the specimen, then a series of elastic and *inelastic scattering* (3.31) process takes place inside the specimen for the incident electrons and generated SEs. Connection of the spatial location of scattering event forms an electron trajectory. Tracking of electron trajectory is terminated when an electron is absorbed by losing its kinetic energy to below *surface barrier* (3.39) or leave from the specimen surface. Calculation includes the determination of free path as a function of energy, the outcome of a scattering event, i.e. the new direction, position and energy of a primary electron and a SE if it is generated.

Note 2 to entry: The simulation for electron beam-specimen interaction is made of the following process (Ding 1996). A primary electron enters into the specimen at an angle α of incidence, which may not be normal to the local surface even for a normal incident beam onto the substrate plane, shall suffer a scattering after flying over a distance of free path. This electron step length obeys an exponential probability distribution where the mean free path is determined by the sum of inverse electron total elastic scattering cross section and electron inelastic mean free path. By MC simulation technique a particular value of variable shall be randomly sampled from a given probability density distribution for a continuous variable or from a probability for a discrete variable with a random number uniformly distributed in the interval of 0-1. In discrete scattering model the property of scattering event being either elastic or inelastic is determined by another random number based on the proportion of elastic scattering or inelastic scattering in the total cross section. If it is elastic the scattering angle is sampled from the differential elastic scattering cross section by a random number. If it is inelastic, the associated energy loss and scattering angle are sampled from the corresponding differential or double-differential inelastic scattering cross sections. The new moving direction after scattering can then be determined to derive the updated coordinates of electron after passing by a new step length (Figure 2). Accompanied with electron energy loss in an inelastic event, one SE will be generated and its information on the energy, position and direction will be stored in a stack so that they could be read out after finishing tracing of an incident electron trajectory. All the simulated electrons, either primary or secondary, shall generate further cascade SEs along their trajectories in the solid target. If the energy of an electron reaching the surface is high enough to overcome the surface barrier it is then emitted from the local surface.

Note 3 to entry: MC simulation of SE image and SE linescan profile is performed by counting number of emitted SEs by calculating a certain number of primary electron trajectories, which are incident onto a location at specimen surface corresponding to an image pixel, and the generated cascade SE trajectories inside the specimen for a primary beam scanning the specimen surface.



Key

- E electron kinetic energy
- S sampled electron flight length
- ΔE sampled electron energy loss in an inelastic scattering event
- θ sampled electron scattering angle (polar angle) in an elastic or inelastic scattering event
- φ sampled electron azimuthal angle in an elastic or inelastic scattering event

Figure 2 — Schematic diagram of Monte Carlo simulation of electron trajectory

3.26 model-based library
MBL

database of calculated SE *linescan profiles* (3.10) with a MC simulation method based on physical modelling of electron beam interaction with a *specimen* (3.19) in the *CD-SEM* (3.3) imaging process, having one-to-one correspondence between the simulated SE linescan profile and a parameter set for geometric modelling of specimen topography and beam condition

3.27 MBL simulator

specific MC simulation model and simulation software for producing a MBL database

3.28 scattering cross section
total scattering cross section

effective area that quantifies the essential likelihood of a scattering event when an incident beam strikes a target object, mathematical description of the probability of a scattering event (elastic or inelastic)

Note 1 to entry: Scattering cross-section is usually measured in units of area.

3.29 differential scattering cross section

cross section which is specified as a function of some final-state variable, such as particle angle and/or energy

3.30**elastic scattering**

deflection of an electron in the Coulomb potential of an atomic nucleus where electron energy transfer is negligible and large-angle deflection is possible because electron mass is much smaller than the mass of the nucleus

Note 1 to entry: Note to entry 1: This type of electron collision is mainly responsible for the electron diffusion in a solid.

3.31**inelastic scattering**

energy loss event of an electron due to its interaction with solid electrons, which resulting in an excitation of electronic state, and accompanied with small angle of deflection.

Note 1 to entry: Note to entry 1: This type of electron collision is responsible for slowing down of incident electrons and the production of SEs.

3.32**inelastic mean free path**

average distance travelled by an electron through a medium before losing energy, mathematical description of the probability of an inelastic scattering event

Note 1 to entry: Inelastic mean free path is usually measured in units of length.

3.33**optical constants**

refractive index $n(\omega)$ and extinction coefficient $k(\omega)$, as functions of photon energy $\hbar\omega$

3.34**dielectric function****dielectric data**

complex function which describes the electrical and optical properties of a material versus wavevector q and photon energy $\hbar\omega$

Note 1 to entry: Dielectric function $\varepsilon(\omega) = \varepsilon_1 + i\varepsilon_2$ relates to refractive index $n(\omega)$ and extinction coefficient $k(\omega)$ through $\varepsilon_1 = n^2 - k^2$ and $\varepsilon_2 = 2nk$.

3.35**energy loss function**

physical quantity describing electron energy loss probability or the differential inelastic *scattering cross section* (3.28), which is given via *dielectric function* (3.34) by $\text{Im}\{-1/\varepsilon(q, \omega)\}$

3.36**optical energy loss function**

energy loss function (3.35) at long wavelength limit, $\text{Im}\{-1/\varepsilon(0, \omega)\}$

3.37**plasmon**

quantum of collective electron oscillations in a metal or a semiconductor

3.38**phonon**

quantum of lattice vibrations in a solid

3.39**surface barrier**

potential barrier that an electron to overcome for emission from a solid into vacuum, being the electron affinity for semiconductors and insulators or the sum of Fermi energy and work function for metals

Note 1 to entry: Surface barrier is usually given in unit of eV.

4 Symbols and abbreviated terms

CD	critical dimension
MBL	model-based library
MC	Monte Carlo
SE	secondary electron
SEM	scanning electron microscope/scanning electron microscopy

5 Generation of Model-based Library (MBL)

A MBL is produced by a comprehensive MC simulation with a MBL simulator for a given combination set of experimental parameters and specimen geometric parameters, which are predetermined by a MBL database developer. MBL is a set of simulated SE linescan profiles with one-to-one correspondence to a specific set of instrument- and sample-related parameters.

NOTE A MBL database developer represents an individual and/or an organization who produces a MBL database by using a MBL simulator in accordance with [Clause 5](#).

5.1 Basic components of a MBL simulator

A complete MBL simulator is made of several components for CD-SEM image simulation (References [\[7\]](#) [\[20\]](#)[\[55\]](#)[\[19\]](#)[\[63\]](#)) by including electron probe model, SE signal generation model and SE signal detection model, which are then denoted as the descriptor of the MBL simulator. The values of the descriptor are noted in the MBL description document file, Model.txt.

5.1.1 Electron probe model

The electron probe intensity profile (i.e. beam shape and probe diameter) influences the CD-SEM image sharpness and hence the linescan profile. The probe diameter is broadened by the aberrations of the objective lens, which is an important instrumental parameter of MBL^[50]^[51]. Electron intensity distribution within the beam is never ideal in practical cases. One approximation is a Gaussian shape with a constant size (spot size), another one is an “hourglass shape” beam with or without asymmetrical above- and under-focus form. Any of these can be non-perpendicular to the sample. Accounting for a couple of degrees of “stray” tilt can further improve the accuracy of MBL.

a) Gaussian beam model

The geometric theory of electron-probe formation assumes Gaussian profile of the probe shape ^[10]^[11], and the distribution in the lateral direction is given by [Formula \(2\)](#):

$$G(x|\sigma_b) = \frac{1}{\sqrt{2\pi}\sigma_b} \exp\left(-\frac{x^2}{2\sigma_b^2}\right) \quad (2)$$

An ideal electron beam assumes the landing spot size on the surface of specimen is zero. By this modelling, specimen geometry is independent of probe size for a MBL data simulation. To minimize the library size, it is recommended to simulate SE linescan profiles only for an ideal electron beam in MBL construction; the Gaussian distributions for different probe sizes can be later used in a convolution procedure to derive linescan profiles corresponding to finite probe sizes in MBL curve matching ^[13].

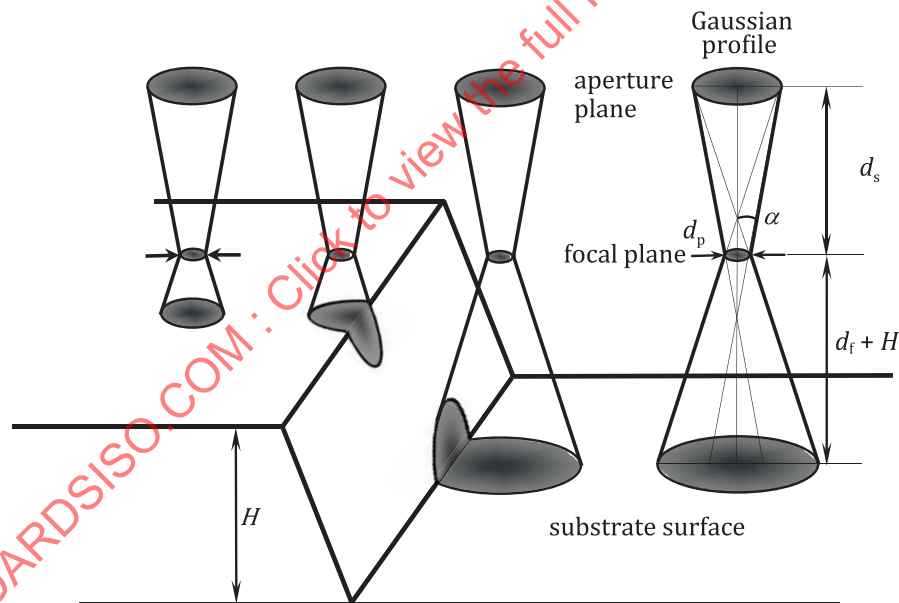
b) Focusing beam model

This model considers an electron beam having a convergence whose angle is defined by the angular aperture^[53]^[62]. At the focal plane electrons are distributed in a certain shape of profile not necessarily follows the exact Gaussian function, having an effective beam width in each of the *x*- and

y-directions. Electrons are more divergently distributed horizontally when arriving on surface if it is away from the focal plane. By this model, the mean direction of the incident electrons is normal to the substrate plane but incident directions of individual electrons may deviate from the mean incident direction. The density distribution of electrons arriving at specimen surface is influenced by the distance away from the focus plane. Therefore, there is no exact definition of electron probe size for landing electrons as it relates to specimen topography. This makes differences on SE emission intensity for incident electrons striking on different locations of a topographic surface, e.g. between the top of the line, the sidewall, and the substrate^{[43][44]}.

The simulation of SE linescan profiles should be carried out for each value set of focusing parameters (Figure 3), i.e. the nominal probe size or effective beam width d_p (nm) which is given on the focal plane, convergence angle α (mrad), working distance d_s (mm), and defocus value d_f (nm) as the distance between the focal plane and the top surface. The focusing position is measured from the specimen top surface where it is defined as the just-focus position (i.e. $d_f = 0$), while $d_f < 0$ and $d_f > 0$ correspond to under-focus and over-focus cases, respectively, where the vertical coordinate is positive along the beam incidence direction. An incident electron trajectory with its incident direction and landing position are determined by random sampling two horizontal positions in aperture plane and focal plane from Gaussian distributions and connecting them as a straight ray towards the landing surface^[62]. At the aperture plane and focal plane, the beam widths are given respectively by $d_s \tan \alpha$ and d_p . The obtained MBL curves are directly matched with the measured one without convolution.

NOTE Focusing beam model excels Gaussian beam model in accuracy of description of SE linescan profiles by adding further three parameters but enlarging greatly the MBL data file size. $d_p = 2\sqrt{2 \ln 2} \sigma_b$ when $\alpha = 0$.



Key

- H height of a trapezoid line
- α convergence angle of incident electron beam
- d_s working distance
- d_f the distance between the focal plane and the top surface
- d_p the effective beam width or the diameter of least confusion disc along the beam axis

Figure 3 — Schematic diagram of focusing electron probe shape at different landing positions of a line structure

5.1.2 SE signal generation model

Primary electrons hitting the specimen surface will diffuse in a specimen through a series of elastic and inelastic scattering processes. The excitation and emission of SEs are the result of these fundamental scattering processes inside the solid specimen. The MC simulation of SEM imaging process is based on a physical model of such electron-solid interaction under various approximations (References [25] [15] [29] [31] [26] [33] [11]). A reasonable physical model of SE signal generation process is essential to a MBL simulator and database construction. The physical model includes the following interaction processes.

a) Elastic scattering

The screened Rutherford cross section was employed in an early MC simulation model of elastic scattering. However, as the spin-orbit coupling becomes increasingly important in the low-voltage region below 1 kV and for heavier elements, which is not taken into account in the Rutherford model, the Mott cross section should be used. Results based on the Mott theory are found in better agreement with the available experimental data for low energy electrons. The differential elastic scattering cross section in the Mott theory^[34] can be obtained numerically by a partial wave expansion method and by solving the relativistic Dirac equation in a central field^{[39][24]}. As Mott cross section is not represented by a specific analytic expression, the calculated numerical values of the differential cross section are stored in a table in a MC program for simulation.

b) Inelastic scattering

There are several different inelastic interaction mechanisms on the fundamental physics of electron inelastic scattering that relates to the SE generation including inner-shell excitation, single electron excitation and plasmon excitation. Among them bulk plasmon is a collective longitudinal oscillation of the electron gas, whose decay can also excite SEs. The unified treatment of these inelastic channels is through the use of dielectric function $\epsilon(q, \omega)$, where $\hbar q$ is momentum transfer and $\hbar \omega$ is energy loss. The differential inverse inelastic mean free path is proportional to the energy loss function, $\text{Im}\{-1/\epsilon(q, \omega)\}$. The energy loss and the associated SE generation in individual scattering events can be treated by MC random sampling^{[14][33]}.

The abundant dielectric data for $\epsilon(0, \omega)$ or optical constants in the loss energy range of $10^0 - 10^4$ eV experimentally measured are available and compiled^{[35][21]}. The advantage to use them is that the electronic excitation in real materials is more accurately described. They are used as the input data to a MC simulation. There are multiple algorithms to extrapolate the optical energy loss function $\text{Im}\{-1/\epsilon(0, \omega)\}$ into the (q, ω) -plane, for example, single pole approximation (SPA), full Penn algorithm (FPA)^[36] and Howie's finite sum by using the plasmon-pole form of Lindhard dielectric function^[41]. The dielectric functional model influences largely the calculated SE energy distribution and absolute SE yield, but may less on the SE linescan profile which is a relative intensity.

Another model of electron inelastic scattering is based on the use of Bethe's stopping power equation under the continuous slowing-down approximation^{[31][49]}. The electron energy loss is evaluated through the multiplication of stopping power and step length between two successive elastic scattering events. As Bethe's stopping power equation is invalid in the low energy region, the Joy's modified equation with an empirical extension to low energy region^[25] is useful. In addition, for free-electron-like materials the plasmon excitation is well-defined and a discrete inelastic scattering model is available^{[5][6]}.

Dielectric functional formalisms (FPA and SPA) are better than the stopping power equation approach under the continuous slowing-down approximation and the discrete scattering channel approach is the more accurate description of electron inelastic scattering and secondary electron signal generation for a wide range of materials; and FPA is superior to SPA.

c) SE generation

According to individual inelastic scattering model (FPA and SPA), the energy loss is transferred to a knock-on electron and to cause a SE generation. The moving direction of the generated SE is assumed to be isotropic. After its birth, the SE will suffer similar elastic and inelastic scattering as

primary electrons and cause cascade production of low energy SEs. Only those emitted electrons into vacuum with their kinetic energies lower than 50 eV are counted as true SE signals^[14]. Individual inelastic scattering models (FPA and SPA) combined with cascade production model can provide reasonable absolute SE yields in agree with experimental data range^{[15][16]}.

In the stopping power equation approach in continuous slowing-down approximation the amount of SE signals for one trajectory within one step length are estimated via energy loss. This approach can only give relative yield-energy dependence and the absolute SE yield determination needs a fitting of multiplication factor by comparing the calculation with experiments.

d) SE emission

When an electron is reaching the surface from interior of a specimen for emission, the refraction of electrons by the surface barrier at the local surface needs to be considered because the surface barrier influences the energy and angular distribution of slow electrons. Two approaches exist for transmission function. The classical one as a step function only requires the kinetic energy is higher than the surface barrier, while the quantum mechanical representation^{[14][27]} gives the varied emission probability depending on the kinetic energy as well as the ejection angle.

NOTE In the case of charging the surface barrier changes as surface electric potential.

e) Phonon scattering

The interaction between an electron and lattice is a process of phonon scattering. The energy of electron changes slightly but the momentum has a significant change; especially at low energies, electrons have high probability to interact with the lattice vibration. This inelastic scattering channel is particularly not negligible for an insulator.

f) Charging of insulating specimen

Charge accumulation with electron beam irradiation can distinctly change electric potential on specimen surface and cause image distortion^[12]. The time variation of electrostatic field between the specimen and detector influences SE trajectories and hence signal intensity. The charging effect evidently affects SE image contrast for insulators and therefore has a potential risk of improper CD evaluation. An implementation of charging effect simulation by a MC method needs to include the following aspects^{[40][28]}.

The charge production, diffusion and deposition in the specimen: negative charges (SEs) and positive charges (holes) are produced in electron inelastic scattering events. They are determined by tracking incoming probe electrons and outgoing SEs and BSEs. The potential and the electric field in the space of inside and outside specimen are calculated by solving the Poisson equation considering the proper boundary conditions based on the charge distribution. The charges then diffuse in the specimen under the electric field. The complex specimen structures, for example rough surface topography, will make charge effect simulation more demanding due to boundary conditions.

Motion of electron trajectories: Established electric field alters the forthcoming electron trajectories, which in turn change the surface electric potential dynamically. This is a self-consistent calculation towards establishing the equilibrium state.

Although MC method can quantitatively simulate charging effect by a suitable physical model for CD evaluation^[28], the charging is a dynamic problem and charge-up of an insulator is a self-regulating process. Because the charging effect relies on beam current and particularly irradiation time, it in fact limits the construction of MBL database by adding more parameters.

5.1.3 SE signal detection model

It is an advantage of the CD-SEM detector that the low-energy SEs can be collected with a high efficiency by a collector grid biased to a positive potential of several hundred volts^[17]. It is intended to prevent the loss of signal associated with low energy SEs re-entering the specimen.

SEs that produced in the beam-specimen interaction process and emitted from the specimen obey cosine law of angular distribution. They travel in straight lines in a space free of electric field and may re-enter the specimen if they meet neighbouring structural surfaces in their movement. In this case the SE signal is shadowed and cannot be counted by a detector, thereby resulting in SE yield reduction. A quantitative detector model is helpful for taking account of the shadowing effect in CD-SEM simulation. It is practical useful to compensate the unknown detector property and detection efficiency by using a parameter p , representing the degree of the extraction by an external field, for a particular type of CD-SEM instrument.

The value of the parameter p is between 0 and 1, where “0” represents the case of no-extraction, and “1” the case of full extraction by a sufficiently high external field. In the no-extraction mode, escaping SEs from the specimen is assumed to travel in straight lines. Electrons leaving the specimen have a chance of being absorbed by the neighbouring structures in their paths. In the full-extraction mode, an SE is detected as soon as it emerges from the specimen surface. In the partial extraction mode, value of this parameter is larger than 0 and smaller than 1; in this case SE signal is extracted with certain probability. In the partial extraction mode, SE signals are extracted with the probability of p and the corresponding image intensity is given by [Formula \(3\)](#):

$$I_p = (1-p)I_{p=0} + pI_{p=1} \quad (3)$$

where $I_{p=0}$ and $I_{p=1}$ represent the intensity of non-extraction and full-extraction, respectively^[55]. For a MBL database construction only $I_{p=0}$ and $I_{p=1}$ are necessary to be included, while the partial extraction intensity can be later calculated in a MBL curve matching procedure.

The detection model records statistics of SE signals emitted into whole space from the incident location of an electron beam scanning over specimen structure at specified pixel size.

5.2 Model of specimen

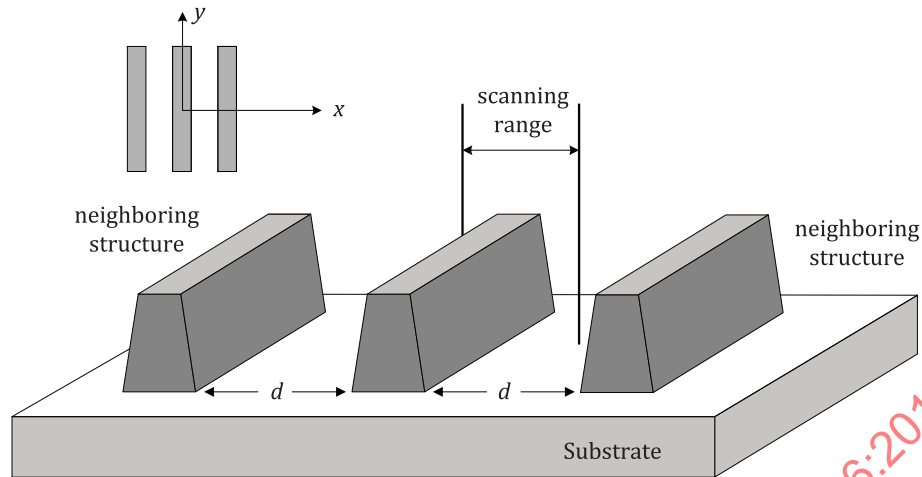
The SE yield increases with tilt angle of the local surface normal in relative to the incident beam (i.e. the SE tilt dependence)^[45] so difference of surface-tilt is one of the main sources of topographic contrast, while another source is shadowing effect. In general, the specimen structure determines the topographic contrast of the SE image.

The model of specimen is the necessary input condition for a MC simulation and MBL database construction. A model of specimen is specified by the shape of its boundary and the properties of the materials it includes. The model parameters are predetermined by a MBL database developer.

5.2.1 Specimen structure and parameters

The simulation specimen space for a line structure contains line structure and substrate. The simulated line structure consists of three identical lines, with the spacing d sited at the same substrate ([Figure 4](#)). Only the simulation result of SE linescan profile for the central line is necessary while the two lines aside are used to include shading effect in no-extraction and partial extraction mode of SE signal detection.

NOTE When the single trapezoid model does not present enough CD performance as in the case of photoresist pattern, use the double trapezoid model.


Key

- d spacing between two trapezoid lines as measured from bottom
 x coordinate axis, which is vertical to a trapezoid line, of linescan profiles
 y axis which is parallel to a trapezoid line

Figure 4 — Specimen geometric structure
a) Single trapezoid model

A single line structure is described in a single trapezoid model by the following parameters: top CD (TCD, T), bottom CD (BCD, B), height (H), right- and left-bottom sidewall angles (SWA, θ_r and θ_l), right- and left-top rounding (TR, R_r^t and R_l^t) and right- and left-bottom rounding (BR, R_r^b and R_l^b). Single line structure can either be symmetric or be asymmetric (Figure 5 a)). In symmetric case, TCD, BCD, H and SWA are related by Formula (4):

$$B - T = 2H \tan \theta \quad (4)$$

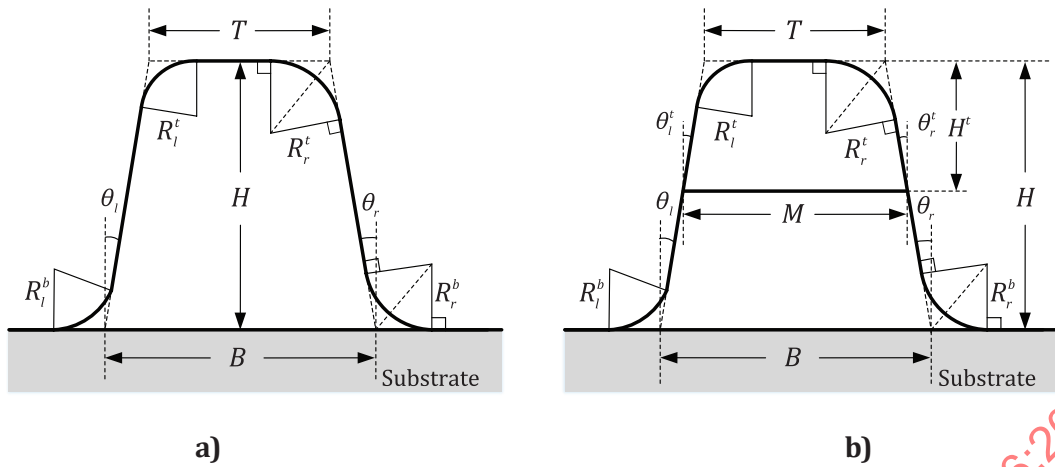
b) Double trapezoid model

A double trapezoid model is more suitable for precise approximation of photoresist profile than a single trapezoid model. A single line structure is described in a double trapezoid model by the following parameters: top CD (TCD, T), middle CD (MCD, M), bottom CD (BCD, B), height (H), top height (H^t), right- and left-bottom sidewall angles (SWA, θ_r and θ_l), right- and left-top sidewall angles (TWSA, θ_r^t and θ_l^t), right- and left-bottom rounding (BR, R_r^b and R_l^b) and right- and left-top rounding (TR, R_r^t and R_l^t). Single line structure can either be symmetric or be asymmetric (Figure 5 b)). In symmetric case, TCD, MCD, BCD, H , H^t , SWA and TWSA are related by the Formulae (5) and (6):

$$M - T = 2H^t \tan \theta^t \quad (5)$$

$$B - M = 2(H - H^t) \tan \theta \quad (6)$$

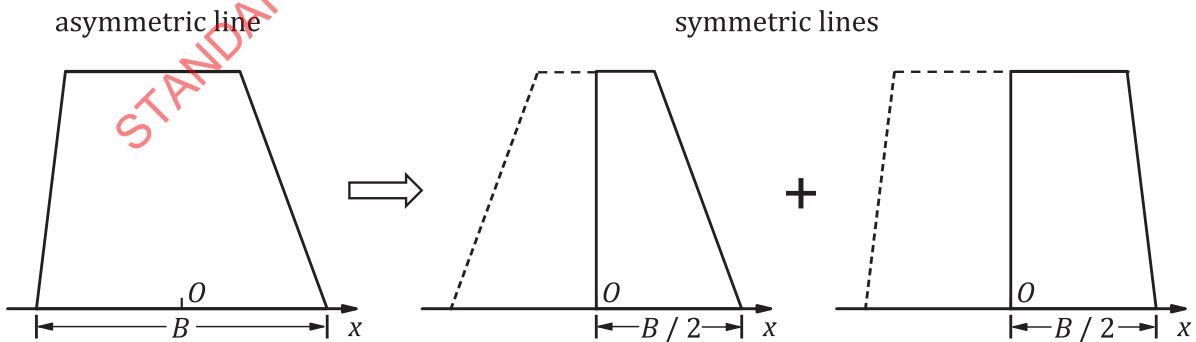
The asymmetric case greatly enlarges the volume of MBL data. In order to reduce the cost of MBL resource, an asymmetric line is approximated by joining two half parts of a simulated symmetric line for different structure parameters (SWA, TR and BR). The scanning range for simulation is set as right half part of the central line, $(0, B/2 + d/2)$, with the origin of horizontal coordinate for the linescan profile set at the midpoint of bottom CD (Figure 6).



Key

- H height of a trapezoid line
- H^t top height of a trapezoid line in double trapezoid model
- T top CD
- M middle CD
- B bottom CD
- θ_r right-bottom sidewall angle
- θ_l left-bottom sidewall angle
- θ_r^t right-top sidewall angle in double trapezoid model
- θ_l^t left-top sidewall angle in double trapezoid model
- R_r^b right-bottom rounding
- R_l^b left-bottom rounding
- R_r^t right-top rounding
- R_l^t left-top rounding

Figure 5 — Geometric parameters of cross section of single line structure: a) single trapezoid model; b) double trapezoid model



Key

- O origin of horizontal axis
- x horizontal axis
- B bottom CD

Figure 6 — Approximating an asymmetric line by symmetric line shape

5.2.2 Specimen specification

The SE yield depends on the atomic number of the specimen but not monotonously^{[45][59]}. For a MC simulation, input parameters of specimen property include elemental composition, density and basic electronic properties: surface barrier and conductivity for insulators (band gap is implicit in the dielectric data for semiconductors).

5.2.3 Generation methods of specimen geometry

Different methods may be used for construction of specimen geometry or surface topography.

a) Constructive solid geometry (CSG)

This method uses basic geometries to build a complex specimen structure with combination of Boolean operations, i.e. union, difference and intersection^{[29][56]}. 3D simple primitives including spheres, cylinders, polyhedral and so on are used to make complex shapes. The primitives are analytically described with a few geometric parameters. Based on this construction, intersecting points of an electron trajectory with a geometry surface can be easily and efficiently determined.

b) Finite element triangular mesh (FETM)

This method generates a mesh that approximates a specimen geometric topography by using elementary triangular planes. The generated mesh is enclosed as specimen boundary. It allows an easy construction of an arbitrary complex structure with smooth or rough surface^{[30][61]}.

There are also other methods used to build expected geometric topography of specimen, for example, tetrahedral mesh method which is similar to FETM method and height maps which is a 2D array of heights on a regularly spaced x - and y -grids.

A trapezoidal line with the circular arc angles and smooth surface are considered for CD metrology by MBL method. Considering the complexity of treatment of electron scattering near the boundary as well as the optimization of simulation, it is recommended CSG and FETM methods for generation of specimen geometric model for MBL database construction. Especially, when charging effect becomes an essential issue in CD metrology simulation for insulator, using FETM method is more conducive. A computer language program or freely available (GNU General Public License) software can be used to automatically and regularly generate specimen line structure library by a MBL database developer.

5.3 Monte Carlo simulation

A MBL database contains series of SE linescan profiles for specified specimen and instrument parameter sets in sequence. The data are obtained by a MC simulation of CD-SEM image for the line structure under the specified input parameters; the data are stored according to the data file structure.

The main MC program treats random sampling of electron scattering events of incident electrons (Ding 1996) and generated SEs with a chosen electron inelastic scattering model (e.g. FPA, SPA or other discrete model) for the considered material defined in a geometric structure (i.e. by FETM or CSG). Sample geometry and material property are defined by subroutines. Specific procedures are as follows:

5.3.1 Input parameters

Input parameters for a MC simulation include: parameters of the specimen geometric structure (i.e. width, height, sidewall angle and rounding), basic material properties (i.e. elemental composition, density, optical dielectric function and electronic properties), parameters of electron beam condition (i.e. primary energy, incident angle, beam size, convergence angle, defocus, and beam current and scanning time per grid for insulating specimen) and parameters for scanning simulation (i.e. scanning range and step).

5.3.2 Beam-specimen interaction

The electron beam is set at incident angles in xz - and yz -planes with respect to the normal direction (z -axis) of the substrate plane (xy -) in the construction of MBL data by a MC simulation. A primary electron beam scans over vertical cross section of a line along x -axis for a range of interest, i.e. the central line in [Figure 4](#) including space aside, in the specimen surface at a specified horizontal grid size. The grid size which may not be the pixel size for imaging is appropriately chosen so that both the resolution and signal to noise ratio of simulated linescan profile are satisfactory for determined number of incident electron trajectories.

Generation method for specimen geometric topography needs to fit to MC procedure for a quick judging of intersection of an electron flight path with a surface or a boundary between two parts of material in a specimen. In addition, the space subdivision method is useful to accelerate the simulation.

For each horizontal grid point a certain number of, usually 10 000 at least, incident electron trajectories are necessary for a MC simulation of linescan profile whose signal to noise ratio is proportional to the inverse square root of the number. The SE yield is obtained when the number of emitted SEs is scaled with the number of incident electron trajectories. Such a calculated SE signal emission intensity curve, i.e. SE yield $Y(x)$ as a function of beam position x will be recorded into a MBL database as a library data. The above steps are repeated for the designed inputs of structure parameters and beam parameters to form a whole MBL database.

5.4 MBL file structure

MBL means a series of data for CD metrology and their organization mode. The method shall provide various functions, such as data input, storage, organization and information retrieval with optimized searching. The data is comprised of parameters about CD-SEM imaging simulation, including instrument condition, specimen specification and geometric structure, and SE linescan profile. The parameters and SE linescan profiles are saved in the MBL file together as a whole.

A MBL database includes files, "Model.txt", a text file for model description, and at least one data file which is a binary file containing simulated SE linescan profiles with corresponding parameter values, together with a parameter specification file, "Parameter.txt". MBL database developer should specify the appropriate values or value ranges with intervals for the listed parameters.

5.4.1 Variable type and value

Parameters with the name, data type, meaning and value are given in the following table.

Variable name	symbol	Variable type	description	value
<i>Data_filename</i>		character string	file names of a related MBL database	
<i>Electron_beam</i>		character string	beam model	"Gaussian beam" or "focus-ing beam"
<i>Elastic_scattering</i>		character string	elastic scattering model	"Mott cross section" or "Rutherford formula"
<i>Inelastic_scattering</i>		character string	inelastic scattering model	"dielectric function (FPA)" or "dielectric function (SPA)" or "continues slow-ing-down" or "discrete ine-lastic channel" or "others" (to be specified)
<i>SE_generation</i>		character string	SE generation model	"cascade" or "others" (to be specified)
<i>SE_emission</i>		character string	SE emission model	"quantum" or "classical" or "others" (to be specified)
<i>Charging</i>		character string	charging modelling	"included" or "not included"

Variable name	symbol	Variable type	description	value
<i>Ref_No</i>		character string	optional reference numbers	
<i>Ref</i>		character string	optional list of references	
<i>Structure</i>		character string	the structure and chemical composition of specimen	
<i>Barrier</i>		real type number	the single value of surface barrier in eV	
<i>Trapezoid</i>		character string	trapezoid model	“single” or “double”
<i>PE</i>	E_p	integer type number	the single value of primary energy in eV	
<i>PE_min</i>		integer type number	the minimum value of the range of primary energy in eV	
<i>PE_max</i>		integer type number	the maximum value of the range of primary energy in eV	
<i>PE_step</i>		integer type number	the step value of the range of primary energy in eV	
<i>IAx</i>	ϑ_x	real type number	the single value of incident angle in xz-plane in deg.	
<i>IAx_min</i>		real type number	the minimum value of the range of incident angle in xz-plane in deg.	
<i>IAx_max</i>		real type number	the maximum value of the range of incident angle in xz-plane in deg.	
<i>IAx_step</i>		real type number	the step value of the range of incident angle in xz-plane in deg.	
<i>IAy</i>	ϑ_y	real type number	the single value of incident angle in yz-plane in deg.	
<i>IAy_min</i>		real type number	the minimum value of the range of incident angle in yz-plane in deg.	
<i>IAy_max</i>		real type number	the maximum value of the range of incident angle in yz-plane in deg.	
<i>IAy_step</i>		real type number	the step value of the range of incident angle in yz-plane in deg.	
<i>BS</i>	d_p	real type number	the single value of beam size (Gaussian model) or optional effective beam width (focusing model) in nm	
<i>BS_min</i>		real type number	the minimum value of the range of beam size (Gaussian model) or optional effective beam width (focusing model) in nm	
<i>BS_max</i>		real type number	the maximum value of the range of beam size (Gaussian model) or optional effective beam width (focusing model) in nm	

Variable name	symbol	Variable type	description	value
<i>BS_step</i>		real type number	the step value of the range of beam size (Gaussian model) or optional effective beam width (focusing model) in nm	
<i>COA</i>	α	real type number	the single value of optional convergence angle (focusing model) in mrad	
<i>COA_min</i>		real type number	the minimum value of the range of optional convergence angle (focusing model) in mrad	
<i>COA_max</i>		real type number	the maximum value of the range of optional convergence angle (focusing model) in mrad	
<i>COA_step</i>		real type number	the step value of the range of optional convergence angle (focusing model) in mrad	
<i>WD</i>	d_s	real type number	the single value of optional working distance (focusing model) in mm	
<i>WD_min</i>		real type number	the minimum value of the range of optional working distance (focusing model) in mm	
<i>WD_max</i>		real type number	the maximum value of the range of optional working distance (focusing model) in mm	
<i>WD_step</i>		real type number	the step value of the range of optional working distance (focusing model) in mm	
<i>DFD</i>	d_f	real type number	the single value of optional defocusing distance in nm	
<i>DFD_min</i>		real type number	the minimum value of the range of optional defocusing distance (focusing model) in nm	
<i>DFD_max</i>		real type number	the maximum value of the range of optional defocusing distance (focusing model) in nm	
<i>DFD_step</i>		real type number	the step value of the range of optional defocusing distance (focusing model) in nm	
<i>TCD</i>	T	real type number	the single value of top CD in nm	
<i>TCD_min</i>		real type number	the minimum value of the range of top CD in nm	
<i>TCD_max</i>		real type number	the maximum value of the range of top CD in nm	
<i>TCD_step</i>		real type number	the step value of the range of top CD in nm	
<i>MCD</i>	M	real type number	the single value of middle CD in nm	
<i>BCD</i>	B	real type number	the single value of bottom CD in nm	

Variable name	symbol	Variable type	description	value
<i>Height</i>	H	real type number	the single value of height in nm	
<i>Height_min</i>		real type number	the minimum value of the range of height in nm	
<i>Height_max</i>		real type number	the maximum value of the range of height in nm	
<i>Height_step</i>		real type number	the step value of the range of height in nm	
<i>TH</i>	H^t	real type number	the single value of top height in nm	
<i>TH_min</i>		real type number	the minimum value of the range of top height in nm	
<i>TH_max</i>		real type number	the maximum value of the range of top height in nm	
<i>TH_step</i>		real type number	the step value of the range of top height in nm	
<i>SWA</i>	θ	real type number	the single value of bottom sidewall angle in deg.	
<i>SWA_min</i>		real type number	the minimum value of the range of bottom sidewall angle in deg.	
<i>SWA_max</i>		real type number	the maximum value of the range of bottom sidewall angle in deg.	
<i>SWA_step</i>		real type number	the step value of the range of bottom sidewall angle in deg.	
<i>TSWA</i>	θ^t	real type number	the single value of top sidewall angle in deg.	
<i>TSWA_min</i>		real type number	the minimum value of the range of top sidewall angle in deg.	
<i>TSWA_max</i>		real type number	the maximum value of the range of top sidewall angle in deg.	
<i>TSWA_step</i>		real type number	the step value of the range of top sidewall angle in deg.	
<i>TR</i>	R^t	real type number	the single value of top rounding in nm	
<i>TR_min</i>		real type number	the minimum value of the range of top rounding in nm	
<i>TR_max</i>		real type number	the maximum value of the range of top rounding in nm	
<i>TR_step</i>		real type number	the step value of the range of top rounding in nm	
<i>BR</i>	R^b	real type number	the single value of bottom rounding in nm	
<i>BR_min</i>		real type number	the minimum value of the range of bottom rounding in nm	
<i>BR_max</i>		real type number	the maximum value of the range of bottom rounding in nm	

Variable name	symbol	Variable type	description	value
<i>BR_step</i>		real type number	the step value of the range of bottom rounding in nm	
<i>Spacing</i>	<i>d</i>	real type number	the single value of line spacing in nm	
<i>Spacing_min</i>		real type number	the minimum value of the range of line spacing in nm	
<i>Spacing_max</i>		real type number	the maximum value of the range of line spacing in nm	
<i>Spacing_step</i>		real type number	the step value of the range of line spacing in nm	
<i>X_min</i>	x_{min}	real type number	the minimum value of x-grid for scanning range in nm	
<i>X_max</i>	x_{max}	real type number	the maximum value of the x-grid for scanning range in nm	
<i>X_step</i>	Δx	real type number	the step value of x-grid for scanning range in nm	
<i>Y_min</i>	Y_{min}	real type number	the minimum value of calculated SE emission yield within the scanning range	
<i>Y_max</i>	Y_{max}	real type number	the maximum value of calculated SE emission yield within the scanning range	

NOTE 1 Default value needs to be appropriately given by MBL database developer unless specified.

NOTE 2 Default value of *Charging* is “not included” for metal and semiconductor.

NOTE 3 Default value of *X_min* is 0., the origin of x-axis, and at the center of the line structure ([Figure 4](#)).

NOTE 4 Default value of *X_max* is set at the center of the right spacing ([Figure 4](#)).

NOTE 5 When *Trapezoid* is “single”, *TH* is set to 0 and the value of *TSWA* equals to *SWA*.

5.4.2 Model description file

Not all of the approximate models are consistently used in any particular simulation; there are different MC models for the same phenomenon by choosing different approximations for beam-specimen interaction. A model description file can then help the MBL software developers and users to identify the approximations used in construction of a particular MBL database. It is a text file named as “Model.txt” in which the model values for focusing beam model, SE generation model and charging model shall be given and the related references are listed afterwards (see [Annex B](#)). The file format is:

“Electron beam =” *Electron_beam Ref_No*

“Elastic scattering =” *Elastic_scattering Ref_No*

“Inelastic scattering =” *Inelastic_scattering Ref_No*

“Secondary electron generation =” *SE_generation Ref_No*

“Secondary electron emission =” *SE_emission Ref_No*

“Charging =” *Charging Ref_No*

Ref

NOTE A MBL software developer represents an individual and/or an organization who develops a MBL software for CD determination in accordance with [Clause 7](#).

5.4.3 Parameter specification file

A parameter specification file is associated with a particular MBL library set, where the measurement condition for simulation is described, which includes, e.g. accelerating voltage, specimen geometric structure and chemical composition, surface barrier, top CD, bottom CD, height, sidewall angle, top rounding and bottom rounding of a trapezoid line. A certain value or the value range of varying parameters is given. It is a text file named as "Parameter.txt" (see [Annex C](#)). The file format is:

"Data filename =" *Data_filename*

"Specimen structure =" *Structure*

"Surface barrier =" *Barrier*, "(eV)"

"Primary energy =" *PE*, or, *PE_min* "-" *PE_max* "at intervals of" *PE_step*, "(eV)"

"Incident angle (xz) =" *IAX*, or, *IAX_min* "-" *IAX_max* "at intervals of" *IAX_step*, "(deg.)"

"Incident angle (yz) =" *IAY*, or, *IAY_min* "-" *IAY_max* "at intervals of" *IAY_step*, "(deg.)"

"Beam size =" *BS*, or, *BS_min* "-" *BS_max* "at intervals of" *BS_step*, "(nm)"

"Convergence angle =" *COA*, or, *COA_min* "-" *COA_max* "at intervals of" *COA_step*, "(mrad)"

"Working distance =" *WD*, or, *WD_min* "-" *WD_max* "at intervals of" *WD_step*, "(mm)"

"Defocusing distance =" *DFD*, or, *DFD_min* "-" *DFD_max* "at intervals of" *DFD_step*, "(nm)"

"Top CD =" *TCD*, or, *TCD_min* "-" *TCD_max* "at intervals of" *TCD_step*, "(nm)"

"Height =" *Height*, or, *Height_min* "-" *Height_max* "at intervals of" *Height_step*, "(nm)"

"Top height =" *TH*, or, *TH_min* "-" *TH_max* "at intervals of" *TH_step*, "(nm)"

"Top sidewall angle =" *TSWA*, or, *TSWA_min* "-" *TSWA_max* "at intervals of" *TSWA_step*, "(deg.)"

"Bottom sidewall angle =" *SWA*, or, *SWA_min* "-" *SWA_max* "at intervals of" *SWA_step*, "(deg.)"

"Top rounding =" *TR*, or, *TR_min* "-" *TR_max* "at intervals of" *TR_step*, "(nm)"

"Bottom rounding =" *BR*, or, *BR_min* "-" *BR_max* "at intervals of" *BR_step*, "(nm)"

"Spacing =" *Spacing*, or, *Spacing_min* "-" *Spacing_max* "at intervals of" *Spacing_step*, "(nm)"

5.4.4 Preparation of library data

Ensure that reasonable agreements with experimental data (Seiler 1983; Joy 1994; Reimer 1998) for MC simulated SE energy distribution, SE angular distribution, SE tilt dependence and SE yield dependence on primary energy by a MC simulator used for MBL simulation have been confirmed for elemental solids.

Normalize the simulated data of SE linescan profiles after an appropriate noise reduction to avoid accidental happened abnormal normalization and matching due to noise by using [Formula \(7\)](#):

$$I_i^{MBL} = \text{int}2 \left[32767 \times \frac{Y(x_i)^{MBL} - Y_{\min}}{Y_{\max} - Y_{\min}} \right], \quad \{i=1, 2, \dots, \text{int}[(x_{\max} - x_{\min})/\Delta x]\} \quad (7)$$

where $\{Y(x_i)^{MBL}\}$ represents a simulated SE linescan profile of the emission yield, Y_{\min} and Y_{\max} are the minimum and maximum SE emission intensity values of the $\{Y(x_i)^{MBL}\}$ -curve from substrate and line structure, respectively. $\{I_i^{MBL}\}$ is the normalized linescan profile.

NOTE $\text{int}2(x)$ is a function for converting a real variable x to a short integer of 2 bytes, $\text{int}(x)$ is a function for converting a real variable x to an integer of 4 bytes.

5.4.5 MBL data structure

The data structure for the data file uses hierarchical model as well as relational model ([Figure 7](#)). The hierarchical model is used to establish the relationship of the data for navigation of beam and signal detection parameters, while the relational model is used to establish the connection between the structure parameters of the specimen and SE linescan profiles.

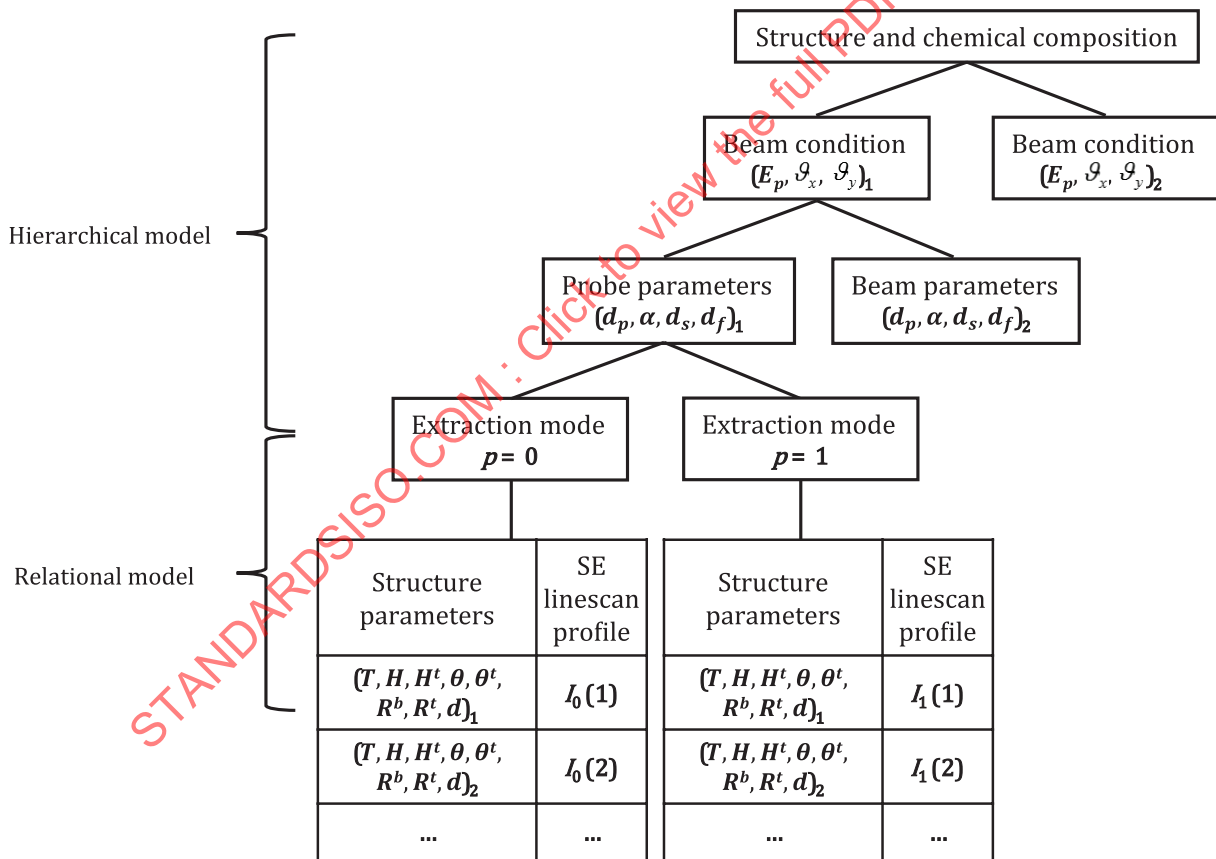


Figure 7 — Schematic of data structure for the data file in a MBL database

5.4.6 MBL data file format

Store all data in the database binary format to ensure the accuracy of data and to reduce the storage space. The file contains a head for specification of number of grid points and the values of x -grids in nm whose origin is set at the middle of central line ([Figures 4](#) and [6](#)) and two ends are set at the middle of space between two lines, number of primary energies and followed by the values in eV, number of

incident angles in xz -plane and followed by the values in deg., number of incident angles in yz -plane and followed by the values in deg., number of beam sizes and followed by the values in nm, number of convergence angles and followed by the values in mrad, number of working distances and followed by the values in mm, number of defocus distances and followed by the values in nm, when charging is not included, and in addition, number of beam currents and followed by the values in nA, number of scanning time per grid in ns when charging is considered.

Each data entry stored is sequenced as, the values of instrument parameter set in relational model $(E_p, \vartheta_x, \vartheta_y, d_p, \alpha, d_s, d_f, p)$, the values of specimen structure parameter set in relational model $(T, H, \theta, H^t, \theta^t, R^b, R^t, d)$, the values of x -grid $(x_{\min}, x_{\max}, \Delta x)$, the absolute minimum and maximum intensity values (Y_{\min}, Y_{\max}) , the normalized SE linescan profile data $\{I_i^{\text{MBL}}\}$ starting from x_{\min} to x_{\max} towards the right side (positive x) of grid, and finally followed by the end of line character (CR/LF).

6 Acquisition of a CD-SEM image

6.1 Acceptable image

CD measurement is based on the SE image observed by a CD-SEM user, and the metrology accuracy depends upon the image quality, which is mainly expressed by image contrast and signal to noise ratio. For CD-SEM image acquisition, it is important to first adjust the microscope to the best condition.

Particular attention shall be paid to the adjustment of the electron probe current and the focus of the electron probe, in order to obtain optimal brightness and contrast with minimum noise. Offset and gain should be adjusted carefully to avoid saturation of the signal. Furthermore, use an image that is as free of astigmatism as possible.

6.2 Specimen tilt

Specimen tilt angle between substrate plane normal and incident beam direction is usually set as 0° in a CD-SEM.

NOTE Some CD-SEMs have functions to tilt specimen or electron beam.

6.3 Image quality

The absence of image distortion and drift needs to be assured beforehand in order to obtain results of good quality.

6.4 Selection of the field of view

Select the field of view so that it completely contains measured area of CD in the specimen and includes at least one line for dense line feature (an array of equal lines and spaces) pattern.

6.5 CD-SEM image data file

CD metrology employs SE intensity linescan profile from an SE image which is directly saved from a CD-SEM and shall be stored in grey digital format. Use non-lossy, i.e. distortion-free storage file type, e.g. LZW compressed TIFF, for the image data file.

7 CD determination

CD-SEM user finds the best fit of the measured SE image of lines with the calculated SE linescan profiles, according to the MBL matching procedure, within the range of the library data to obtain the CD values. SE image and basic imaging information including the chemical composition of specimen and primary beam energy is provided by CD-SEM operator for the CD determination.

7.1 Determination of pixel size

Calculate the pixel size L_p (in nm) based on scale marker as in [Formula \(8\)](#):

$$L_p = L_{scale} / N_{scale} \tag{8}$$

where L_{scale} is the “indicator” value (e.g. the nominal value, in nm) of the scale marker on the image, N_{scale} is the number of horizontal pixels covering the length of the scale marker.

NOTE The accuracy of the result depends on scale calibration by using traceable certified reference material. The step is not required once the pixel size is known and meets the reasonable measurement accuracy. It is more accurate to use the information from the image-file header.

7.2 Selection of the field of interest

For CD evaluation select the field of interest in the image, which is vertically along the edge direction with the length L and is horizontally from the middle of the left spacing to the middle of the right spacing across a line structure. The selected image of $(2K + 1) \times N$ pixels, where $N = L/L_p$, is then vertically segmented into a series of horizontal cross sections with a step length ΔL ([Figure 8](#)), and the number of the cross sections is $n = L/\Delta L$ and at least $n \geq 10$. Usually, $\Delta L = L_p$ and $n = N$.

NOTE The measured image of a line structure should be firstly rectified to set the image of aligned lines are parallel to the vertical direction if an image is not taken with a well-controlled CD-SEM imaging system.

7.3 Coordination and normalization

To fit with the data in a MBL database, set the origin of horizontal coordinate of the line image to center of a line. The horizontal coordinate then becomes $x_i = iL_p$, ($i = -K \dots, 0, \dots, K$). The measured SE linescan profiles are then obtained as $Y(x_i)_j^{exp}$ by recording the grayscale intensity for the j th ($j = 1, \dots, n$) vertical cross section. Take the average of image intensity along the line to derive the mean measured SE linescan profiles^[55] shown in [Formula \(9\)](#):

$$\bar{Y}_i^{exp} = \frac{1}{n} \sum_{j=1}^n Y(x_i)_j^{exp} \tag{9}$$

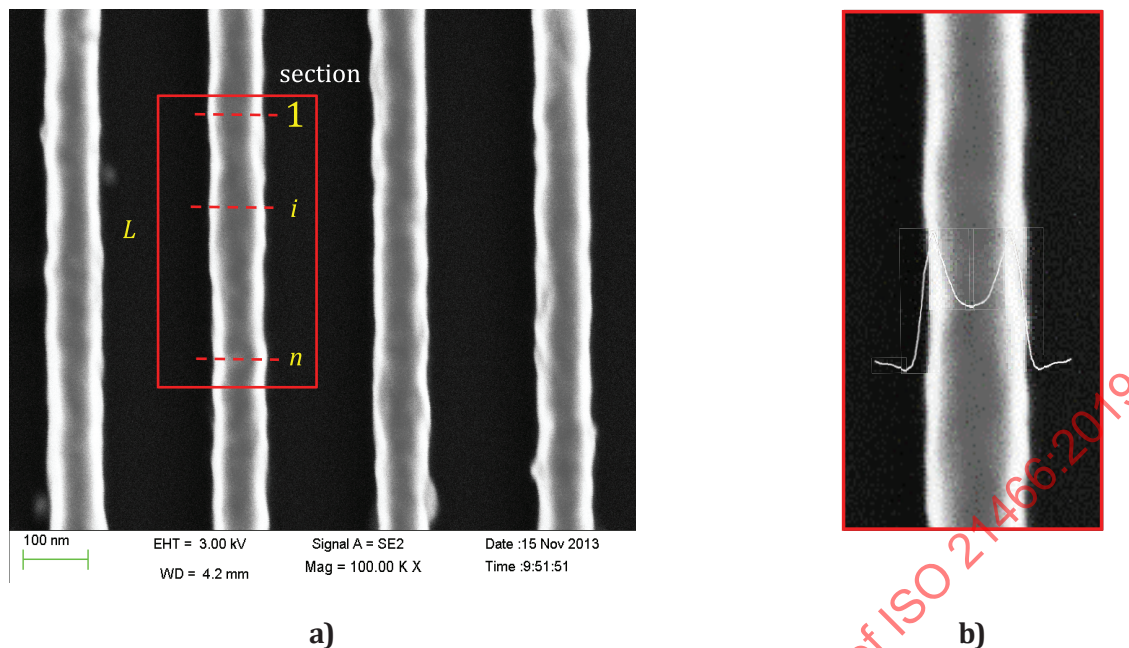
This curve may be smoothed further by an appropriate noise reduction to avoid accidentally happened abnormal normalization and matching due to noise. Perform normalization of intensity according to [Formula \(10\)](#):

$$I_i^{exp} = \frac{(\bar{Y}_i^{exp} - \bar{Y}_{min}^{exp})}{(\bar{Y}_{max}^{exp} - \bar{Y}_{min}^{exp})} \tag{10}$$

where

\bar{Y}_{min}^{exp} and \bar{Y}_{max}^{exp} are the minimum and maximum detected SE emission intensity values of \bar{Y}_i^{exp} ($i = -K, \dots, 0, \dots, K$) from substrate and line, respectively, within the field of interest;

I_i^{exp} is the normalized result.



Key

- L vertical length of the field of interest selected
- 1 the first cross section
- i the i -th cross section
- n the last cross section

Figure 8 — a) Selected field of interest, which is segmented into a series of cross sections along a line structure. b) SE linescan profiles are obtained by gray scale analysis for each cross section, and averaging is taken to derive the mean SE linescan profile.

7.4 Matching procedure

There are two kinds of parameters characterizing a MBL database: specimen ones and instrumental ones. Some parameters are known and fixed in experiment, for example, accelerating voltage, working distance, chemical composition etc. Those known parameters can help to reduce the searching space of the library before matching, which will ensure to derive the results more quickly and efficiently. For convenience the unknown specimen and instrumental parameter sets that to be determined by matching procedure are respectively represented by $S = (T, H, \theta, H^t, \theta^t, R^b, R^t, d)$ and $I = [\vartheta_x, \vartheta_y, \sigma_b \text{ or } (d_p, \alpha, d_s, d_f), p]$ hereafter.

7.4.1 Interpolation

As the horizontal coordinate $\{x_i\}$ counted by the position of pixels and pixel size in the measured image may differ from that in a MBL database, perform an interpolation beforehand for $\{I_i^{\text{exp}}\}$ so that its x -coordinate agrees with that of the MBL database for curve matching according to the value of scanning range and gridding step of scanning range given in the parameter specific file.

7.4.2 Convolution

In MBL database construction the electron probe size can be set to 0, and hence the vanishing defocus value and convergence angle, when a Gaussian model is adopted (see 5.1.1) and the effect of probe size can be computed in matching procedure to minimize the file size of MBL file at cost of longer matching time.

For the Gaussian beam model, the related unknown parameter is σ_b . Perform convolution for each MBL linescan profile $I^{\text{MBL}}(x|\mathcal{S}, I(\sigma_b=0))$ in a MBL database with a Gaussian distribution function $G(x|\sigma_b)$ to derive $I^{\text{MBL}}(x|\mathcal{S}, I(\sigma_b))$ for various values of σ_b by [Formula \(11\)](#)^[22]:

$$I^{\text{MBL}}(x|\mathcal{S}, I(\sigma_b)) = I^{\text{MBL}}(x|\mathcal{S}, I(\sigma_b=0)) * G(x|\sigma_b) \tag{11}$$

[Formula \(12\)](#) depicts the discretized convolution formula:

$$I^{\text{MBL}}(x_i|\mathcal{S}, I(\sigma_b)) = \sum_j I^{\text{MBL}}(x_j|\mathcal{S}, I(\sigma_b=0)) G(x_i - x_j|\sigma_b) \tag{12}$$

where the Gaussian kernel is shown in [Formula \(13\)](#):

$$G(x_i - x_j|\sigma_b) = \frac{1}{\sqrt{2\pi}\sigma_b} \exp\left\{-\frac{(x_i - x_j)^2}{2\sigma_b^2}\right\}. \tag{13}$$

For the focusing beam model, the related unknown parameter set is (d_p, α, d_s, d_f) . When charging is considered, the probe size σ_b shall be non-vanishing in [5.4](#) and this step is unnecessary.

7.4.3 Matching

Use a least square method to search for the optimal fitting result of parameter set by a repetitive matching process. When the available MBL is of small size the library traversing over the entire parameter space is possible to find the global minimum of fitting error. Otherwise, use the Powell's conjugate direction method^[38] to find the minimum values of the sum of residual squares. A computer language program or freely available software can be used.

There are two matching modes, relative scaling and absolute scaling, according to the type of model intensity $I^{\text{mod}}(x)$ used to fit $I^{\text{exp}}(x)$.

An interpolation is performed to derive linescan profile $I^{\text{MBL}}(x|\mathcal{S}, I)$ for various values of extraction probability p by [Formula \(14\)](#):

$$I^{\text{MBL}}(x|\mathcal{S}, I(p)) = (1 - p)I^{\text{MBL}}(x|\mathcal{S}, I(p=0)) + pI^{\text{MBL}}(x|\mathcal{S}, I(p=1)) \tag{14}$$

7.4.3.1 Relative scaling

Use the normalized linescan profile $I^{\text{MBL}}(x)$ as the modelling intensity $I^{\text{mod}}(x)$ in [Formula \(15\)](#):

$$I^{\text{mod}}(x|\mathcal{S}, I) = I^{\text{MBL}}(x|\mathcal{S}, I) \tag{15}$$

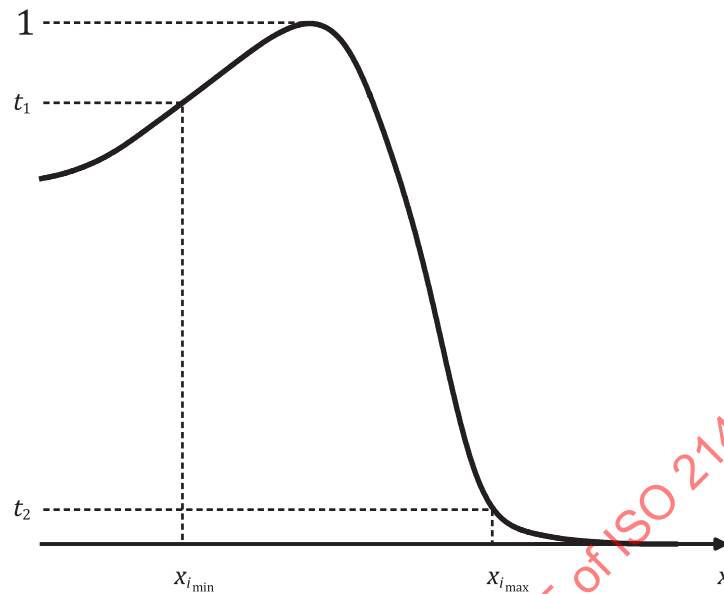
a) Matching right edge:

At a known primary energy E_p , calculate the sum of residual squares in fitting to the right edge of an asymmetrical line as shown in [Formula \(16\)](#):

$$\delta = \frac{1}{i_{\text{max}} - i_{\text{min}}} \sum_{i=i_{\text{min}}}^{i_{\text{max}}} (I_i^{\text{exp}} - I_i^{\text{mod}})^2 \tag{16}$$

and by running over the value ranges of specimen and instrumental parameter sets in a MBL database, where i_{min} and i_{max} are respectively the starting (in the line inner side) and ending (in the edge outer side) grid points for curve matching. Choosing appropriate thresholds t_1 and t_2 for determination of i_{min} and i_{max} by $I_{i_{\text{min}}}^{\text{exp}} = t_1$ and $I_{i_{\text{max}}}^{\text{exp}} = t_2$, respectively, are useful so that the fitting is performed mainly for

the bloom region of SE emission intensity nearby the edge where the intensity changes rapidly ([Figure 9](#)), in order to reduce the fitting error contributed from the region of insignificance.



Key

- 1 unity, the maximum value of normalized intensity
- t_1 first threshold
- t_2 second threshold
- i_{\min} starting position corresponding to the first threshold
- i_{\max} ending position corresponding to the second threshold
- x horizontal axis

Figure 9 — Setting of thresholds for least square fitting

Perform matching firstly in sequence of three parameters, i.e. T , H and θ , which are more sensitive than others.

If δ reaches the global minimum, the corresponding structure in the MBL library represents the measured structure. Obtain the CD values for the right edge (positive x) as shown in [Formula \(17\)](#):

$$(T, H, \theta, H^t, \theta^t, R^b, R^t, d)_r = (T, H, \theta, H^t, \theta^t, R^b, R^t, d)^{\text{MBL}} \quad (17)$$

together with the value of instrumental parameters $[\vartheta_x, \vartheta_y, \sigma_b$ or $(d_p, \alpha, d_s, d_f), p]$.

b) Matching left edge:

Fixing the same value of instrumental parameter set $[\vartheta_x, \vartheta_y, \sigma_b \text{ or } (d_p, \alpha, d_s, d_f), p]$, repeat the above procedure for the left edge (negative x) using the calculation shown in [Formula \(18\)](#):

$$\delta = \frac{1}{i_{\max} - i_{\min}} \sum_{i=i_{\min}}^{i_{\max}} (I_{-i}^{\text{exp}} - I_{-i}^{\text{mod}})^2 \quad (18)$$

and obtain the CD values for the left edge as shown in [Formula \(19\)](#):

$$(T, H, \theta, H^t, \theta^t, R^b, R^t, d)_l = (T, H, \theta, H^t, \theta^t, R^b, R^t, d)^{\text{MBL}} \quad (19)$$

If $H_r \neq H_l$ and/or $H_r^t \neq H_l^t$ within a defined tolerance, repeat the matching (16) and (18) for respectively right- and left-edges by using the mean values, $\bar{H} = (H_r + H_l)/2$ and/or $\bar{H}^t = (H_r^t + H_l^t)/2$, as for searching initial or fixed parameters.

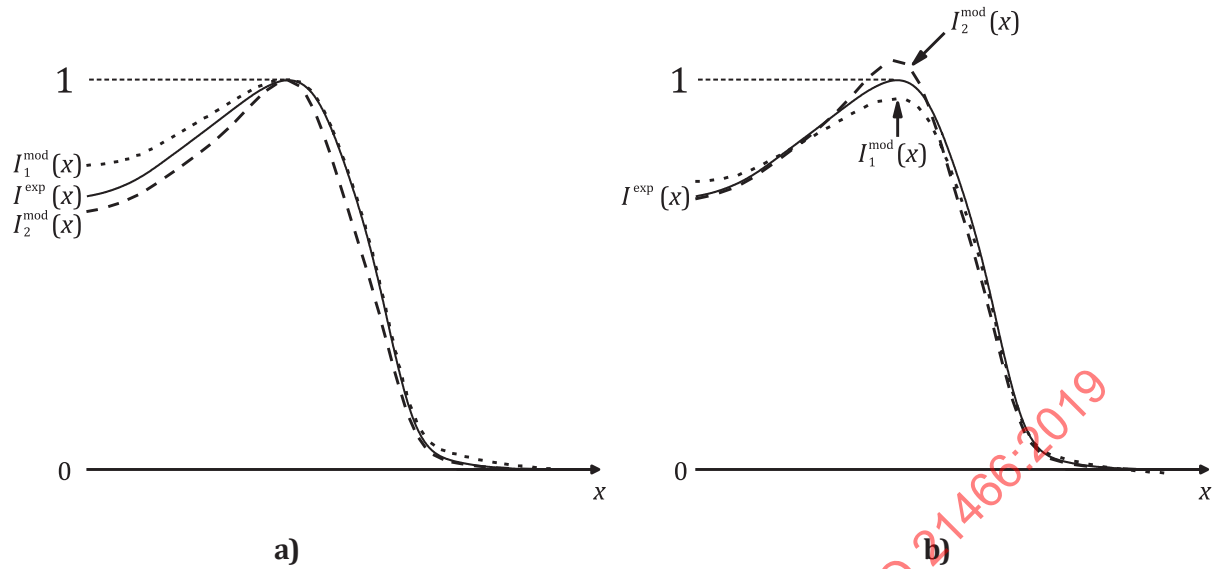
7.4.3.2 Absolute scaling

If $T < 40$ nm, use the scaled linescan profiles [Formula \(20\)](#) (see [Figure 10](#)), as the modelling intensity:

$$I^{\text{mod}}(x|S, l) = a(Y_{\max} - Y_{\min})I^{\text{MBL}}(x|S, l) + b \quad (20)$$

for the further refinement of specimen parameters $(T, H, \theta, H^t, \theta^t, R^b, R^t, d)$, where $Y_{\min} = Y_{\min}(S, l)$ and $Y_{\max} = Y_{\max}(S, l)$ are respectively the minimum and maximum values of one MBL linescan profile as that obtained in [5.4.6](#), and a and b are respectively scaling and offset constant parameters^[48], which are independent of specimen and instrumental parameters.

Fixing the instrumental parameters $[\vartheta_x, \vartheta_y, \sigma_b \text{ or } (d_p, \alpha, d_s, d_f), p]$ as that obtained in relative scaling mode, perform matching (16) and (18), where a and b need also to be determined from the best fitting by using Powell's conjugate direction method, to obtain CD values by (17) and (19) for respectively right- and left-edges.

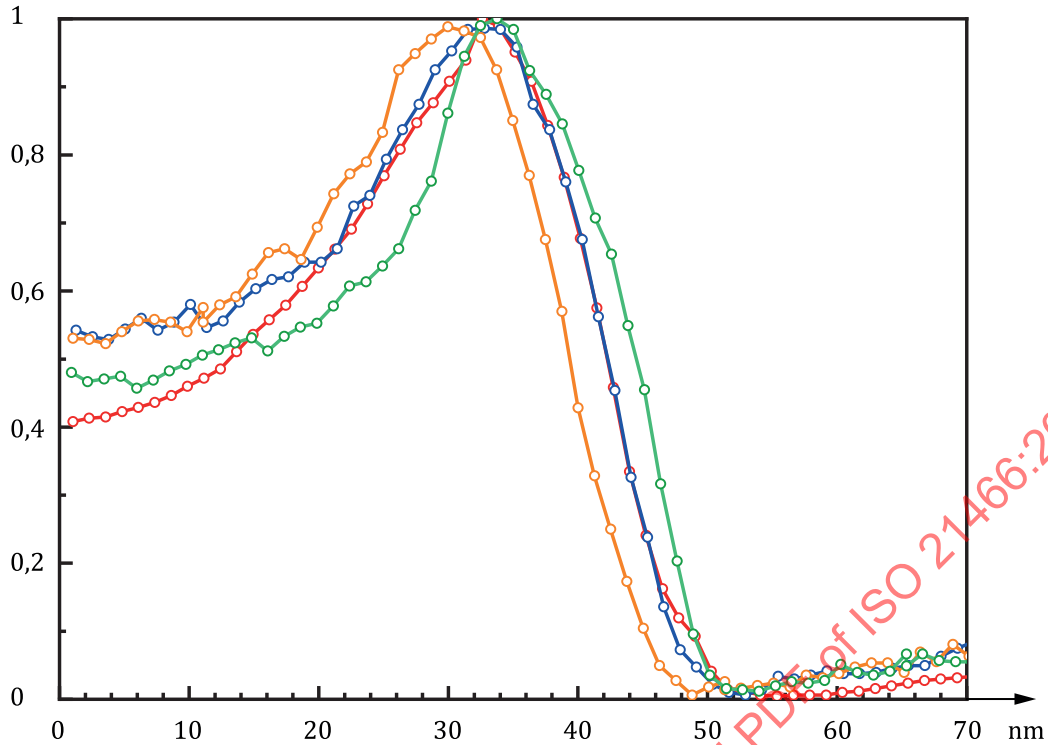
**Key**

- 0 zero, the minimum value of intensity
- 1 unity, the maximum value of normalized intensity
- x horizontal axis
- $I^{\text{exp}}(x)$ normalized experimental linescan profile
- $I_1^{\text{mod}}(x)$ a modelling linescan profile
- $I_2^{\text{mod}}(x)$ a modelling linescan profile

Figure 10 — Comparison of the a) relative scaling mode with the b) absolute scaling mode

Plot the SE linescan profiles for three structures having the close minimum δ -values in a figure for visual identification ([Figure 11](#)).

Precaution is necessary for possible multiple solutions of the parameter set within fluctuation of measured linescan profiles. In case of multiple solutions are found for quite different CD values, perform evaluation at a different primary energy to remove the unlikely parameter sets when necessary. Changing the thresholds, t_1 and t_2 , is helpful to ascertain the more reasonable structure.



Key

- Exp normalized experimental linescan profile
- 1st the matched MBL linescan profile with the minimum sum of residual squares
- 2nd the matched MBL linescan profile with the second minimum sum of residual squares
- 3rd the matched MBL linescan profile with the third minimum sum of residual squares

Figure 11 — Comparison of the averaged experimental SE linescan profile with the three best fitted curves of a MBL database through least square fitting

7.4.4 Averaging

a) Evaluating BCD and MCD:

For the single trapezoid model, evaluate the BCD from right and left sides as in [Formula \(21\)](#):

$$(B-T)_{r,l} = 2H_{r,l} \tan \theta_{r,l} \tag{21}$$

For the double trapezoid model, evaluate the MCD firstly from right and left sides as in [Formula \(22\)](#):

$$(M-T)_{r,l} = 2H_{r,l}^t \tan \theta_{r,l}^t \tag{22}$$

and then evaluate the BCD from right and left sides as in [Formula \(23\)](#):

$$(B-M)_{r,l} = 2(H-H^t)_{r,l} \tan \theta_{r,l} \tag{23}$$

a) Evaluating mean CD:

Obtain the final CD values by taking averages over two sides, shown in [Formulae \(24\) to \(26\)](#):

$$T = (T_r + T_l) / 2 \tag{24}$$

$$B = (B_r + B_l) / 2 \quad (25)$$

$$H = (H_r + H_l) / 2 \quad (26)$$

Calculate the mean CD, D , by taking the mean of TCD and BCD, shown in [Formula \(27\)](#):

$$D = (T + B) / 2 \quad (27)$$

for single trapezoid model (see [Annex D](#)), and weighted by the respective heights of top and bottom parts as:

$$D = \frac{1}{2}(T + B) + \frac{1}{2} \frac{H^t}{H} (M - T) \quad (28)$$

for double trapezoid model in [Formula \(28\)](#).

NOTE The mean CD is middle CD for single trapezoid model, $D = M$.

8 Module functions and relationship

[Figure 12](#) indicates the relationship between different modules and the related stakeholders (i.e. MBL database developer, MBL software developer and CD-SEM user). MBL database module includes MBL simulator, model of specimen, Monte Carlo simulation and MBL database, which are developed by a MBL database developer. MBL software module includes CD-SEM image processing and linescan profile matching, which are implanted into a MBL software developed by a MBL software developer and used by a CD-SEM user, leading to CD determination. CD-SEM image module includes the acquisition of a CD-SEM image by a CD-SEM user.

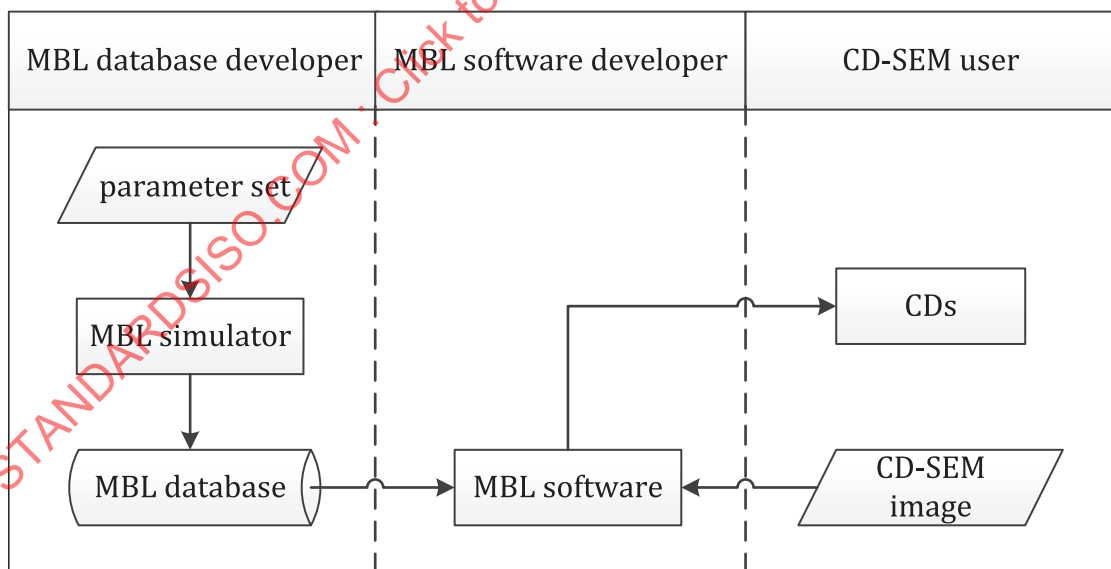


Figure 12 — Flow chart of the relationship between different modules and stakeholders

[Figures 13](#) and [14](#) show respectively brief flow charts of the MBL database module and of the MBL software module. More detailed flow charts for procedures are given in [Annex A](#).

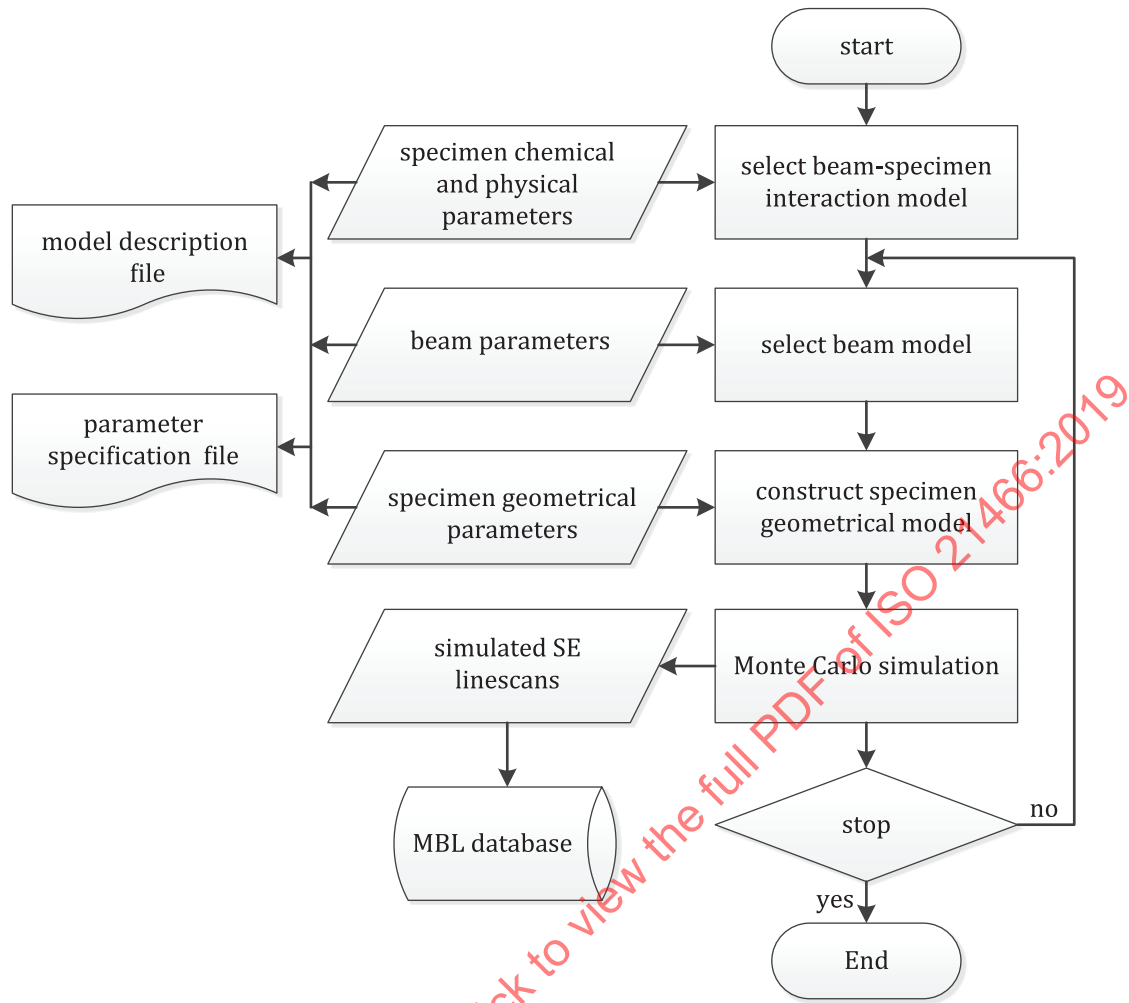


Figure 13 — Flow chart of the MBL database module

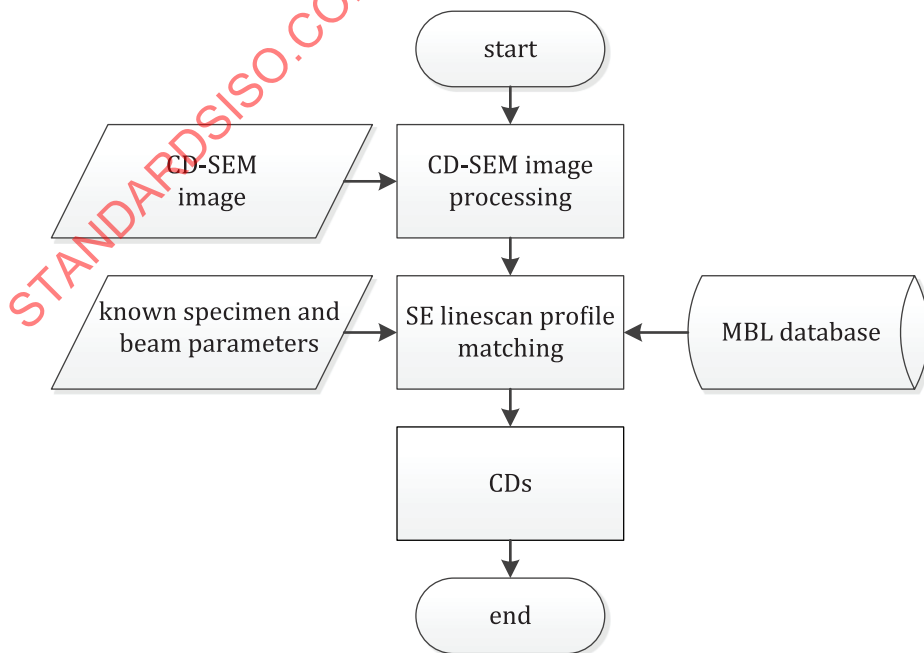


Figure 14 — Flow chart of the MBL software module

9 Uncertainty of CD measurement

The MBL method based on physical models retains the physical basis of CD-SEM imaging, the measured CD data can be confirmed with cross-sectional SEM and TEM observations^{[8][57]}. The inherent error of the measurement relates to the principles relied upon. The measurement error for the CD by using the MBL method will be quantified with uncertainty^[9].

A model is a mathematical approximation of the physical object and may have incorrect assumptions made by omitting some factors. Different MC physical models can be used to describe the beam-specimen interaction, leading to different SE absolute yields and contrast. The divergence on the physical modelling is one possible source of the measurement errors by the MBL method, especially for the modelling of electron inelastic scattering and SE generation.

Another important part of the error is due to the structural modelling as the real structure shape may be distorted from single trapezoid model or double trapezoid model and structure may not be completely described by the adopted structural parameters. For example, the surface roughness has not been included in the modelling. In the MC simulation and MBL database construction, one should also pay attention to the resolution of structural parameters, linescan gridding and statistical intensity fluctuation. The more precise structure modelling, higher resolution and less signal noise can reduce this part of error.

In CD evaluation process with least square method when the minimum residual sum of squares is reached the best fit CDs are obtained for the optimum modeled structure; however, CDs for other structures may results in similar value of residual sum of squares. The matching process may also lead to errors in the measurement.

The combined standard uncertainty $u_C(z)$ of an output measurand z , where z represents one of CDs given by [Formulae \(29\) to \(32\)](#), is expressed as (see ISO/IEC Guide 98-3):

$$u_C^2(z) = u_{\text{MBL}}^2(z) + u_{\text{exp}}^2(z) + u_{\text{mat}}^2(z) \quad (29)$$

The variance of the MBL database module is given by:

$$u_{\text{MBL}}^2(z) = u_{\text{MC-mod}}^2(z) + u_{\text{MC-sim}}^2(z) + u_{\text{spe}}^2(z) \quad (30)$$

where

$u_{\text{MC-mod}}^2$ is the variance due to inaccurate physical modelling in the procedures of beam-specimen interaction as described in [5.1](#) and [Figure A.1](#);

u_{spe}^2 is the variance due to inaccurate specimen geometrical modelling in the procedures of beam-specimen interaction as described in [5.2](#) and [Figure A.1](#);

$u_{\text{MC-sim}}^2$ is the variance due to statistical fluctuation associated with Monte Carlo simulation of linescan profiles in the procedures as described in [5.3](#) and [Figure A.2](#).

The variance of the CD-SEM image module is given by:

$$u_{\text{exp}}^2(z) = u_{\text{image}}^2(z) + u_{\text{scale}}^2(z) \quad (31)$$

where

u_{image}^2 is the variance due to experimental factors affecting image quality in [Clause 6](#); and

u_{scale}^2 is the variance associated with the scale in [7.1](#).

The variance of the MBL software module is given by:

$$u_{\text{mat}}^2(z) = u_{\text{ave}}^2(z) + u_{\text{fit}}^2(z) \quad (32)$$

where

u_{ave}^2 is the variance associated with the averaging of linescan profiles in the procedures of CD determination as described in 7.3 and [Figure A.3](#);

u_{fit}^2 is the variance for the least-square fitting in the procedures of CD determination as described in [7.4.3](#) and [Figure A.3](#).

STANDARDSISO.COM : Click to view the full PDF of ISO 21466:2019

Annex A (normative)

Flow charts of procedures

This annex provides detailed flow charts for the routines appeared in the module described in [Clause 8](#).

[Figure A.1](#) shows flow chart of the procedures for setting beam-specimen interaction model in the MBL database module as described in [5.1](#) and [5.2](#). [Figure A.2](#) shows flow chart of the procedures of Monte Carlo simulation in the MBL database module as described in [5.3](#). [Figures A.3](#) shows flow chart of the procedures of CD determination in the MBL software module as described in [Clause 7](#).

STANDARDSISO.COM : Click to view the full PDF of ISO 21466:2019

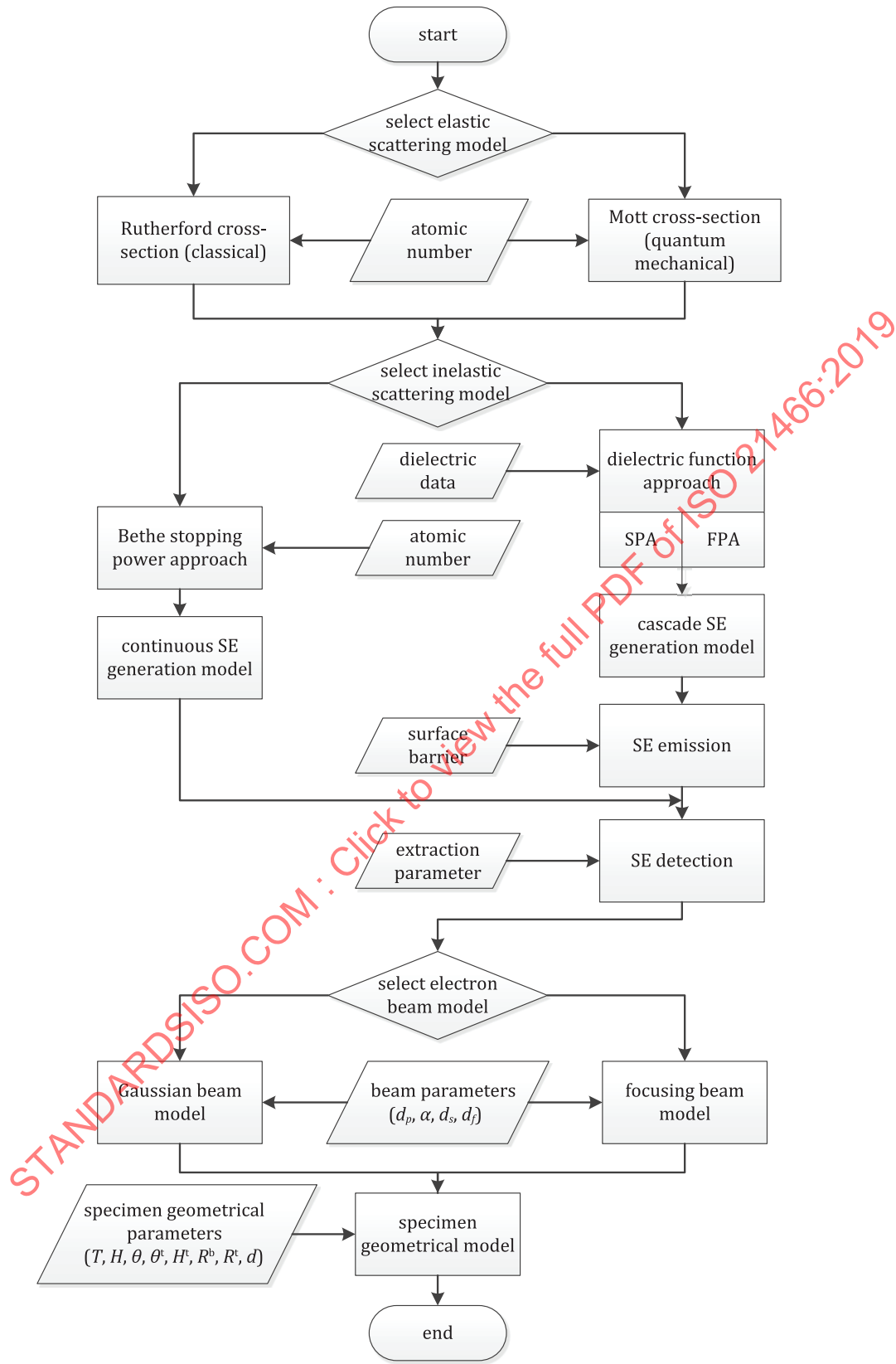


Figure A.1 — Flow chart of the procedures for setting beam-specimen interaction model in the MBL database module

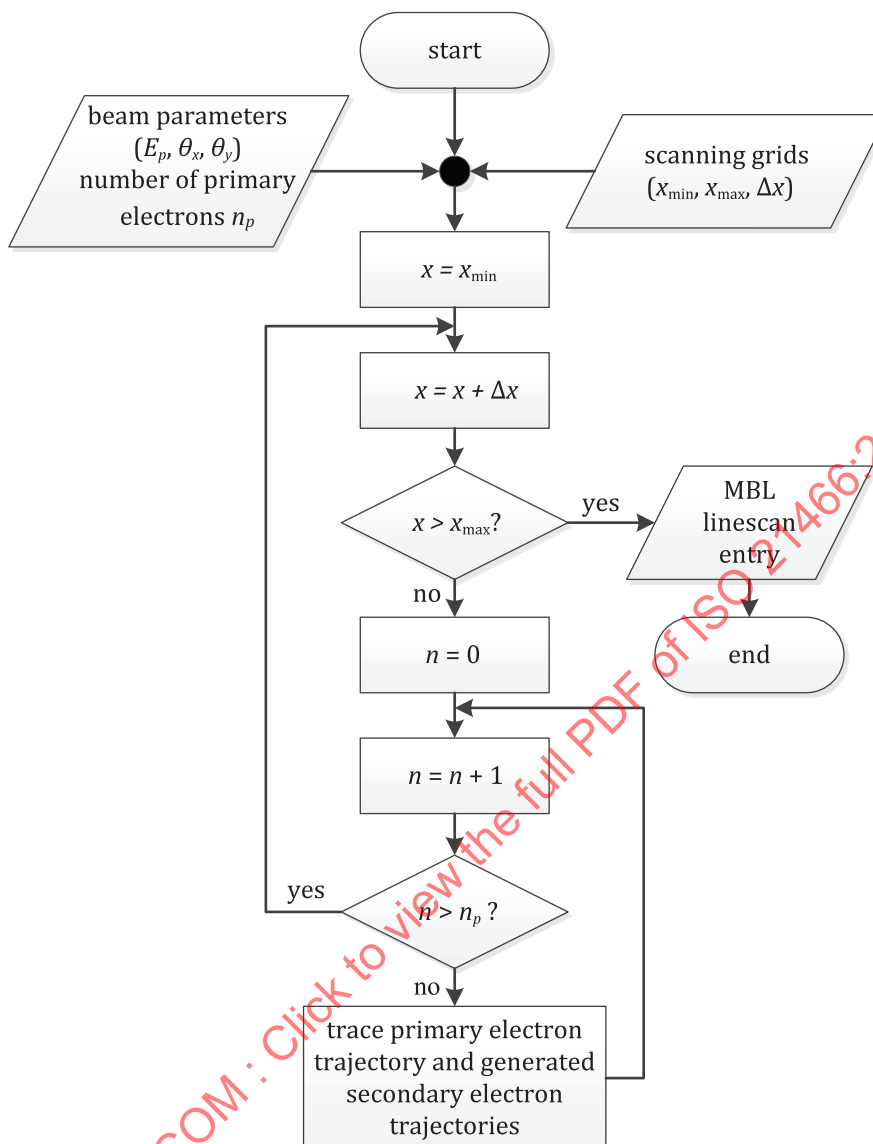


Figure A.2 — Flow chart of the procedures of Monte Carlo simulation in the MBL database module